

Supporting Information

Rhodomyrtals A-D, four unusual phloroglucinol-sesquiterpene adducts from *Rhodomyrtus psidioides*

Qingyao Shou,^{*,a} Joshua E. Smith,^a Htwe Mon,^b Zlatko Brkljača,^c Ana-Sunčana Smith,^{c,d} David M. Smith,^{c,d} Hans J. Griesser,^b Hans Wohlmuth^a

^aSouthern Cross Plant Science, Southern Cross University, PO Box 157, Lismore NSW 2480, Australia

^bIan Wark Research Institute, University of South Australia, Mawson Lakes SA 5095, Australia

^c Institute for Theoretical Physics, Friedrich Alexander University Erlangen-Nürnberg, Nägelsbachstrasse 49b, Erlangen, 91052, Germany

^dRuđer Bošković Institute, Bijenička 54, 10000 Zagreb, Croatia

Tel: +61-2-66203159. Fax: +61-2-66223459. E-mail: sanqi_0617@126.com

List of Supporting Information

- S3. General Experimental Procedures
- S3. Plant Material
- S3. Extraction and Isolation of rhodomyrtal A-D
- S5. ^1H and ^{13}C NMR Spectroscopic Data of rhodomyrtal A-D
- S6. UV spectrum of rhodomyrtal A
- S6. IR spectrum of rhodomyrtal A
- S7. HR-ESI Mass spectrum of rhodomyrtal A
- S8. ^1H NMR spectrum of rhodomyrtal A in pyridine- d_5
- S9. ^1H - ^1H COSY spectrum of rhodomyrtal A in pyridine- d_5
- S10. HMBC spectrum of rhodomyrtal A in pyridine- d_5
- S11. HSQC spectrum of rhodomyrtal A in pyridine- d_5
- S12. NOESY spectrum of rhodomyrtal A in pyridine- d_5
- S13. ^{13}C JMOD spectrum of rhodomyrtal A in pyridine- d_5
- S14. UV spectrum of rhodomyrtal B
- S14. IR spectrum of rhodomyrtal B
- S15. HR-ESI Mass spectrum of rhodomyrtal B
- S16. ^1H NMR spectrum of rhodomyrtal B in pyridine- d_5
- S17. ^1H - ^1H COSY spectrum of rhodomyrtal B in pyridine- d_5
- S18. HMBC spectrum of rhodomyrtal B in pyridine- d_5
- S19. HSQC spectrum of rhodomyrtal B in pyridine- d_5
- S20. NOESY spectrum of rhodomyrtal B in pyridine- d_5
- S21. ^{13}C JMOD spectrum of rhodomyrtal B in pyridine- d_5
- S22. UV spectrum of rhodomyrtal C
- S22. IR spectrum of rhodomyrtal C
- S23. HR-ESI Mass spectrum of rhodomyrtal C
- S24. ^1H NMR spectrum of rhodomyrtal C in pyridine- d_5
- S25. ^1H - ^1H COSY spectrum of rhodomyrtal C in pyridine- d_5
- S26. HMBC spectrum of rhodomyrtal C in pyridine- d_5
- S27. HSQC spectrum of rhodomyrtal C in pyridine- d_5
- S28. ^{13}C JMOD spectrum of rhodomyrtal C in pyridine- d_5
- S29. UV spectrum of rhodomyrtal D
- S29. IR spectrum of rhodomyrtal D
- S30. HR-ESI Mass spectrum of rhodomyrtal D
- S31. ^1H NMR spectrum of rhodomyrtal D in pyridine- d_5
- S32. ^1H - ^1H COSY spectrum of rhodomyrtal D in pyridine- d_5
- S33. HMBC spectrum of rhodomyrtal D in pyridine- d_5
- S34. HSQC spectrum of rhodomyrtal D in pyridine- d_5
- S35. ^{13}C JMOD spectrum of rhodomyrtal D in pyridine- d_5
- S36. The theoretical methodology of CD calculations

S3. General Experimental Procedures

CD spectra were measured on a Jasco J-815 CD Spectopolarimeter at room temperature. UV spectra were measured on a Hewlett Packard 8453 polarimeter at room temperature. IR spectra were recorded on a Bruker Tensor 27 FT IR spectrometer. High resolution electrospray ionisation (HRESIMS) accurate mass measurements were carried out on a Bruker micrOTOF-Q instrument with a Bruker ESI source. NMR spectra were acquired on a Bruker AVANCE 500 MHz spectrometer with TMS as the internal standard. Column chromatography (CC) separations were carried out using MCI gel CHP20P (Supelco, Bellafonte, PA, USA) and Sepra C18-E (50 μm , 65A; Phenomenex Torrance, CA, USA). Preparative HPLC was performed on a Gilson 322 system with a UV/Vis-155 detector and a FC204 fraction collector using a Phenomenex Luna 5 μm (150 \times 21.2 mm i.d.) C-18 column.

S3. Plant Material

The leaves of *Rhodomyrtus psidioides* were collected from a cultivated plant in the Medicinal Plant Garden at Southern Cross University, Lismore, Australia (28° 49' S, 153° 18' E) in April 2012 and authenticated by one of the authors (H.W.). A voucher specimen (PHARM120543) has been deposited in the Medicinal Plant Herbarium at Southern Cross University.

S3. Extraction and Isolation

The dried leaves of *R. psidioides* (600 g) were powdered and extracted with 90% ethanol at room temperature. The ethanol extract was suspended in H₂O and extracted in successive steps using CHCl₃ and EtOAc. The CHCl₃ portion was evaporated under reduced pressure to afford a crude extract (60.2 g). The crude CHCl₃ extract was subjected to MCI gel (CHP20P) Column Chromatography (CC), eluted with a gradient of MeOH/H₂O (70:30 – 90:10) to give seven fractions (A – G). Fraction A (0.7 g) was subjected on a C18 column (5 \times 40 cm) with MeOH/H₂O (7:3–9:1) to give four subfractions (AI–AV). Subfraction AIII (52.9 mg) was

separated by preparative HPLC [Phenomenex Luna C₁₈ column (150 × 21.20 mm) 5 μm; mobile phase acetonitrile and H₂O containing 0.05% TFA (0–5 min: 70% acetonitrile, 5–17 min: 70%-95% acetonitrile, 17–20min: 95% acetonitrile); flow rate 20 mL/min; UV detection at 210 and 280 nm] to give compound **4** (23 mg). Fraction B (3.8 g) was subjected on a C18 column (5 × 40 cm) with MeOH/H₂O (4:1) to give four subfractions (BI–BV). Subfraction BI (290 mg) was separated by preparative HPLC with the same method as AIII to give compounds **3** (21 mg) and **5** (41 mg). Subfractions BIV and V were applied to the preparative HPLC with the same method as AIII to give compounds **1** (78 mg) and **2** (62 mg), respectively.

Rhodomyrtal A (1): a yellow oil; CD λ_{\max} (MeOH) $\Delta\varepsilon_{212}$ -1.97, $\Delta\varepsilon_{268}$ +1.28, $\Delta\varepsilon_{293}$ -0.92, $\Delta\varepsilon_{343}$ -0.82; UV λ_{\max} (MeOH) ($\log \varepsilon$) 203.0 nm (3.93), 278.0 nm (4.13), 386.0 nm (3.42); IR (neat) ν_{\max} : 2932, 1616, 1457, 1436, 1374, 1307, 1188, 886 cm⁻¹; ¹H and ¹³C NMR (Table 1); HRESIMS *m/z* 471.2759 [M - H]⁻ (calcd 471.2747 for C₂₈H₃₉O₆); APCIMS *m/z* 471.1 [M - H]⁻

Rhodomyrtal B (2): a pale yellow oil; CD λ_{\max} (MeOH) $\Delta\varepsilon_{211}$ -3.65, $\Delta\varepsilon_{266}$ +1.10, $\Delta\varepsilon_{290}$ -1.30, $\Delta\varepsilon_{343}$ -1.00; UV λ_{\max} (MeOH) ($\log \varepsilon$) 204.0 nm (4.27), 278.0 nm (4.41), 386.0 nm (3.57); IR (neat) ν_{\max} : 2932, 1617, 1457, 1436, 1365, 1311, 1197, 885 cm⁻¹; ¹H and ¹³C NMR (Table 1); HRESIMS *m/z* 471.2756 [M - H]⁻ (calcd 471.2747 for C₂₈H₃₉O₆); APCIMS *m/z* 471.1 [M - H]⁻.

Rhodomyrtal C (3): a yellow oil; UV λ_{\max} (MeOH) ($\log \varepsilon$) 202.0 nm (3.86), 216.0 nm (3.80), 289 nm (3.78), 386.0 nm (3.35); IR (neat) ν_{\max} : 2933, 1735, 1616, 1457, 1374, 1311, 1204, 887 cm⁻¹; ¹H and ¹³C NMR (Table 1); HRESIMS *m/z* 457.2592 [M - H]⁻ (calcd 457.2590 for C₂₇H₃₇O₆); APCIMS *m/z* 457.1 [M - H]⁻.

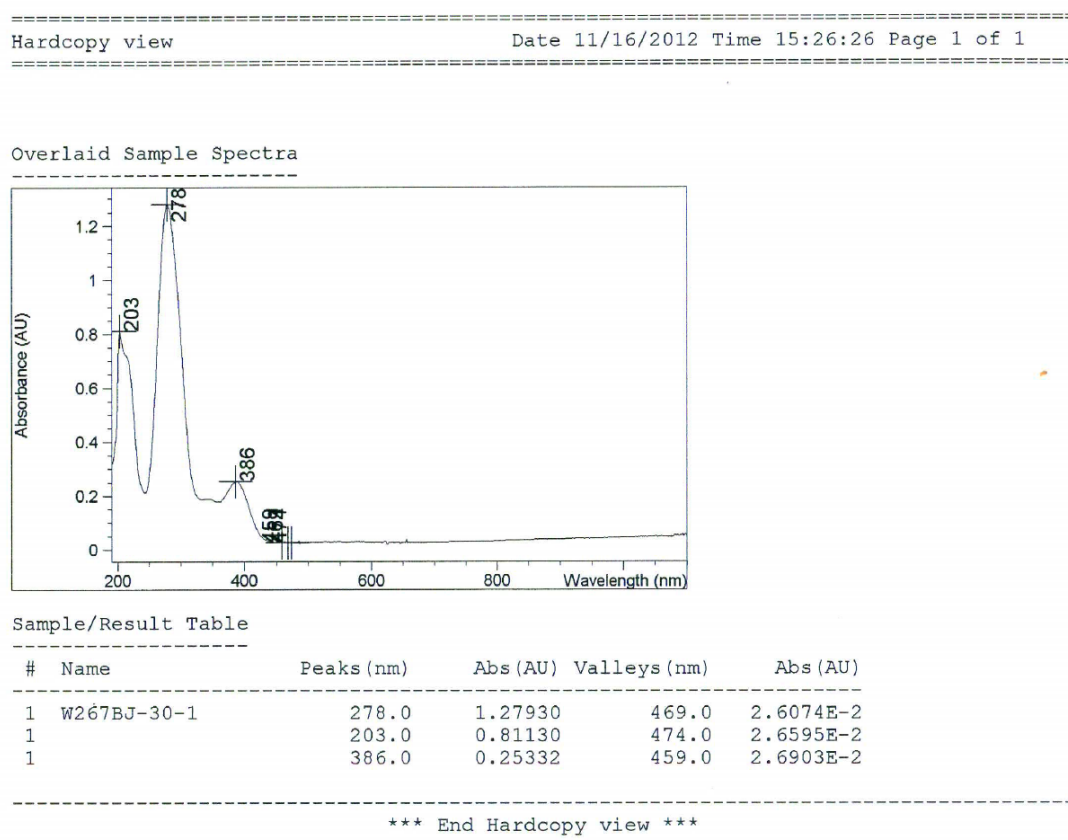
Rhodomyrtal D (4): a yellow oil; CD λ_{\max} (MeOH) $\Delta\varepsilon_{213}$ -5.15, $\Delta\varepsilon_{242}$ +1.04, $\Delta\varepsilon_{271}$ -1.21, $\Delta\varepsilon_{329}$ +0.89, $\Delta\varepsilon_{373}$ -0.50; UV (MeOH) λ_{\max} ($\log \varepsilon$) 203.0 (4.08), 225.0 (3.95), 243.0 (3.87),

278.0 (3.77), 339.0 (3.87) nm; IR (neat) ν_{max} : 3465, 2970, 1739, 1708, 1653, 1624, 1616, 1468, 1439, 1365, 1219, 1218, 1204 cm^{-1} ; ^1H and ^{13}C NMR (Table 1); HRESI-MS m/z 471.3107 [M - 1] $^-$ (calcd for $\text{C}_{29}\text{H}_{43}\text{O}_5$, 471.3110); APCI-MS m/z 471.1 [M-1] $^-$

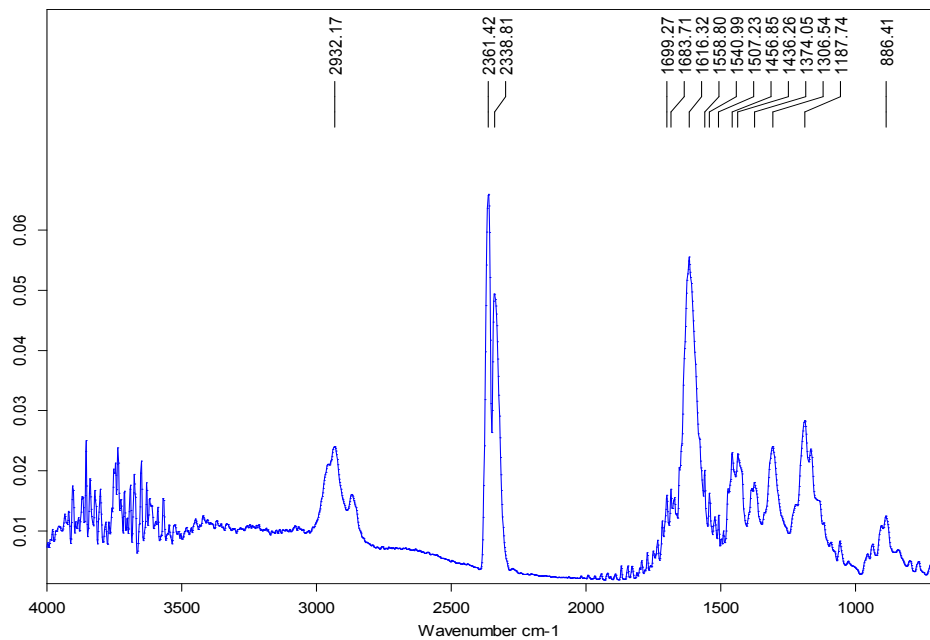
S 5. **Table 1.** ^1H and ^{13}C NMR Spectroscopic Data of Rhodomyrtals A-D (**1-4**) in Pyridine- d_5

	1		2		3		4	
No.	δ_{H}	δ_{C}	δ_{H}	δ_{C}	δ_{H}	δ_{C}	δ_{H}	δ_{C}
1	1.80, m	49.5	1.77, m	49.6	1.80, m	49.6	1.76, m	49.3
2	α , 1.80, m β , 1.67, overlap	26.2	α , 2.25, m β , 1.73, m	24.3	α , 1.82, m β , 1.69, overlap	26.3	α , 1.82, m β , 1.66, overlap	26.2
3	α , 2.01, m β , 1.72, m	44.5	α , 1.93, m β , 1.50, m	42.7	α , 1.99, m β , 1.68, overlap	44.5	α , 2.00, m β , 1.73, m	44.4
4		71.3		71.1		71.3		71.3
5	1.67, overlap	56.6	1.21, m	53.9	1.68, overlap	56.6	1.62, overlap	56.6
6	α , 2.46, m β , 1.42, m	27.0	α , 1.94, m β , 1.86, m	27.1	α , 2.46, m β , 1.44, m	26.9	α , 2.42, m β , 1.42, m	26.9
7	2.05, m	47.0	2.09, m	47.1	2.03, m	46.9	2.00, m	46.9
8	α , 1.67, m β , 1.49, m	27.8	α , 1.70, m β , 1.58, m	28.0	α , 1.66, m β , 1.46, m	27.9	α , 1.65 m β , 1.40, m	27.9
9	α , 2.19, m β , 1.45, m	42.1	α , 2.21, m β , 1.45, m	40.8	α , 2.20, m β , 1.45, m	42.1	α , 2.17, m β , 1.42, m	42.1
10		38.5		38.3		38.5		38.5
11		151.5		151.7		151.5		151.5
12	α , 4.88, s β , 4.81, s	108.8	α , 4.89, s β , 4.80, s	109.0	α , 4.88, s β , 4.81, s	108.8	α , 4.84, s β , 4.77, s	108.7
13	1.77, s	21.5	1.78, s	21.2	1.77, s	21.6	1.74, s	21.5
14	0.92, s	15.1	1.31, s	14.9	0.81, s	15.1	0.91, s	15.1
15	1.28, s	23.6	1.29, s	31.2	1.27, s	23.6	1.24, s	23.5
1'		169.6		169.4		170.0		197.4
2'		105.5		105.4		105.7		106.6
3'		172.5		172.5		173.5		189.7
4'		108.9		109.2		107.0		107.9
5'		167.1		167.1		166.8		179.4
6'		106.7		106.5		108.2		49.2
7'		206.9		206.9		211.3		203.1
8'	3.18, m	53.4	3.17,d, (6.6)	53.4	4.27, m	39.6	3.17, m	49.2
9'	2.40, m	25.7	2.41, m	25.6	1.29, overlap	19.8	2.35, m	26.5
10'	1.03, d (6.6)	23.3	1.03, d (6.6)	23.3	1.29, overlap	19.8	1.02, d (6.7)	23.3
11'	1.03, d (6.6)	23.3	1.03, d (6.6)	23.3			1.02, d (6.7)	23.4
12'	α , 3.06, m β , 2.71, m	22.8	α , 3.13, m β , 2.83, m	23.2	α , 3.07, m β , 2.72, m	22.8	α , 2.92, m β , 2.58, m	22.9
13'	10.54, s	193.2	10.53	193.3	10.58	193.3	1.70, s	25.5
14'							1.66, s	25.6

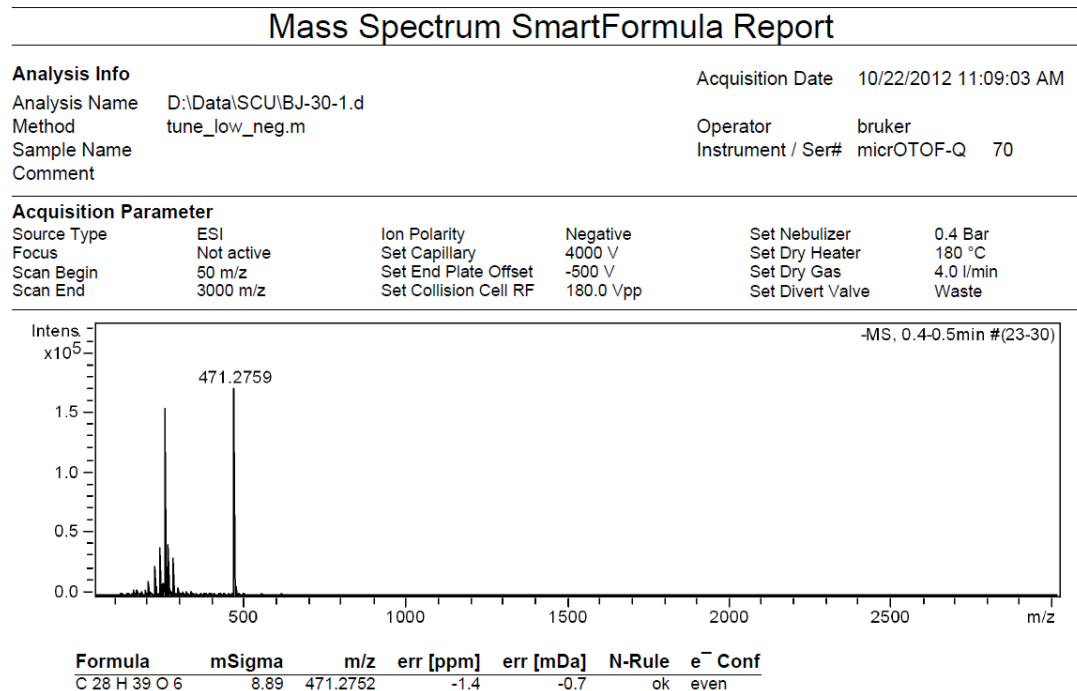
S6. UV spectrum for rhodomyrtal A in methanol



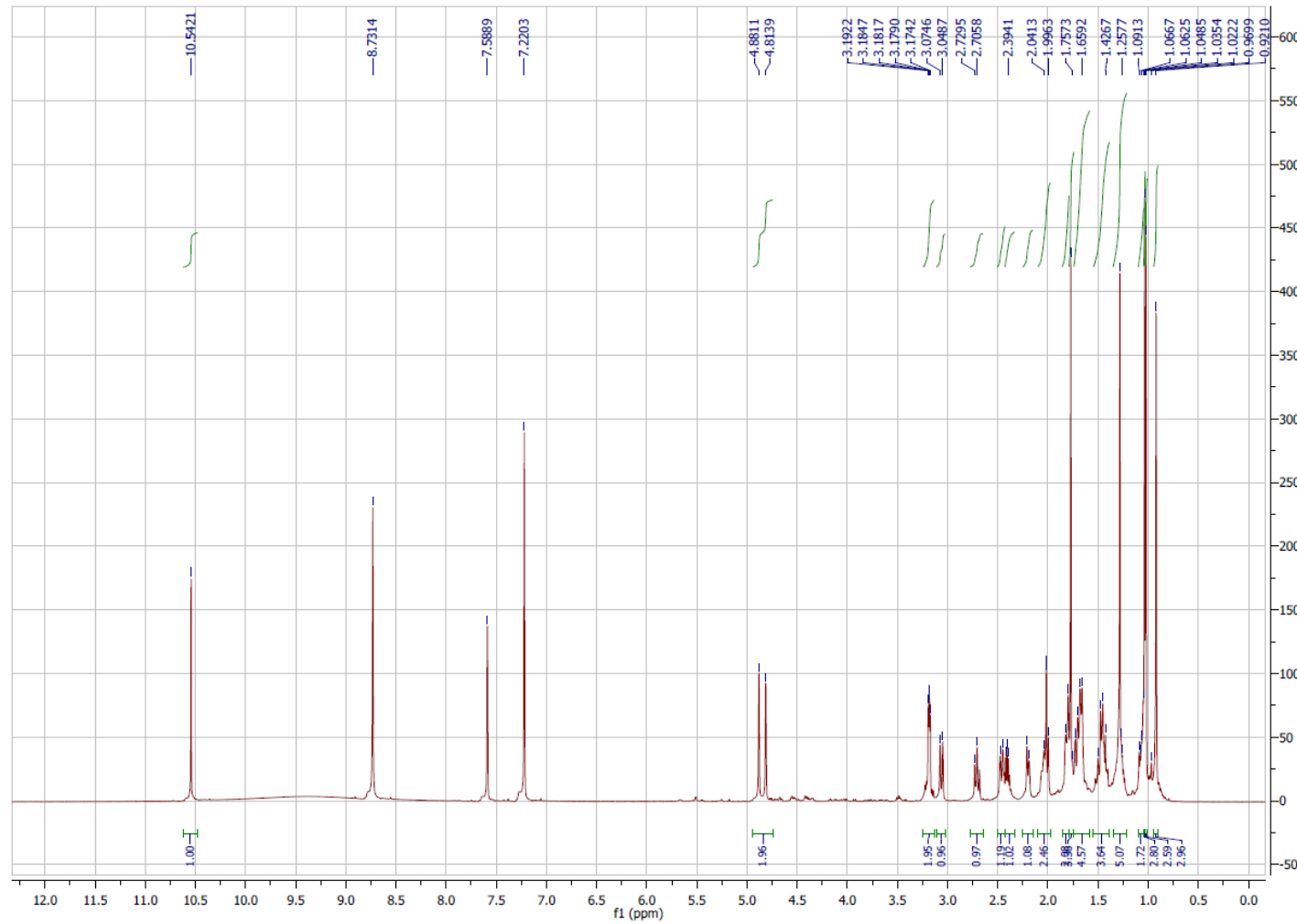
S6. IR spectrum for rhodomyrtal A



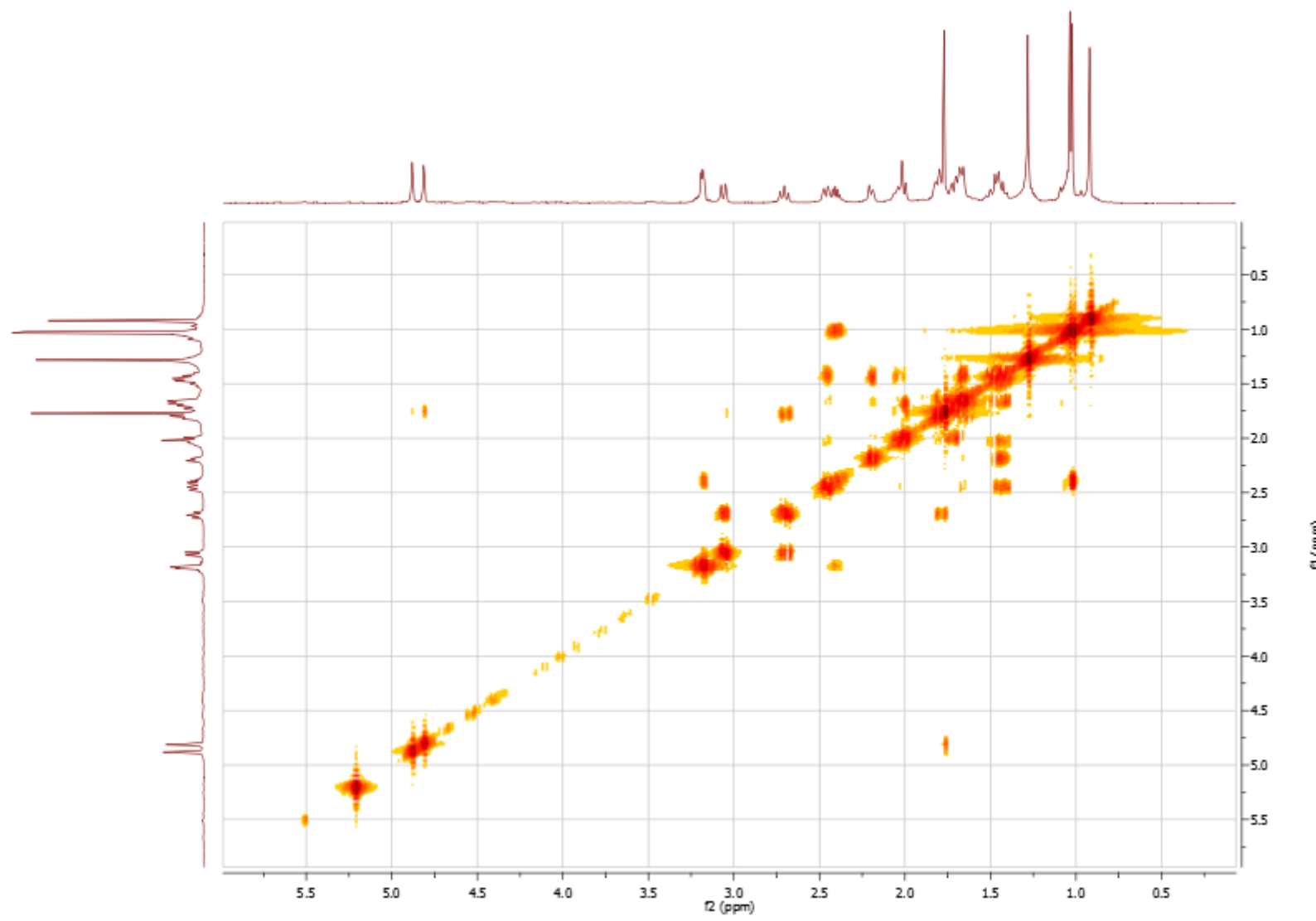
S7. HR-ESI Mass spectrum (negative) of rhodomyrtal A



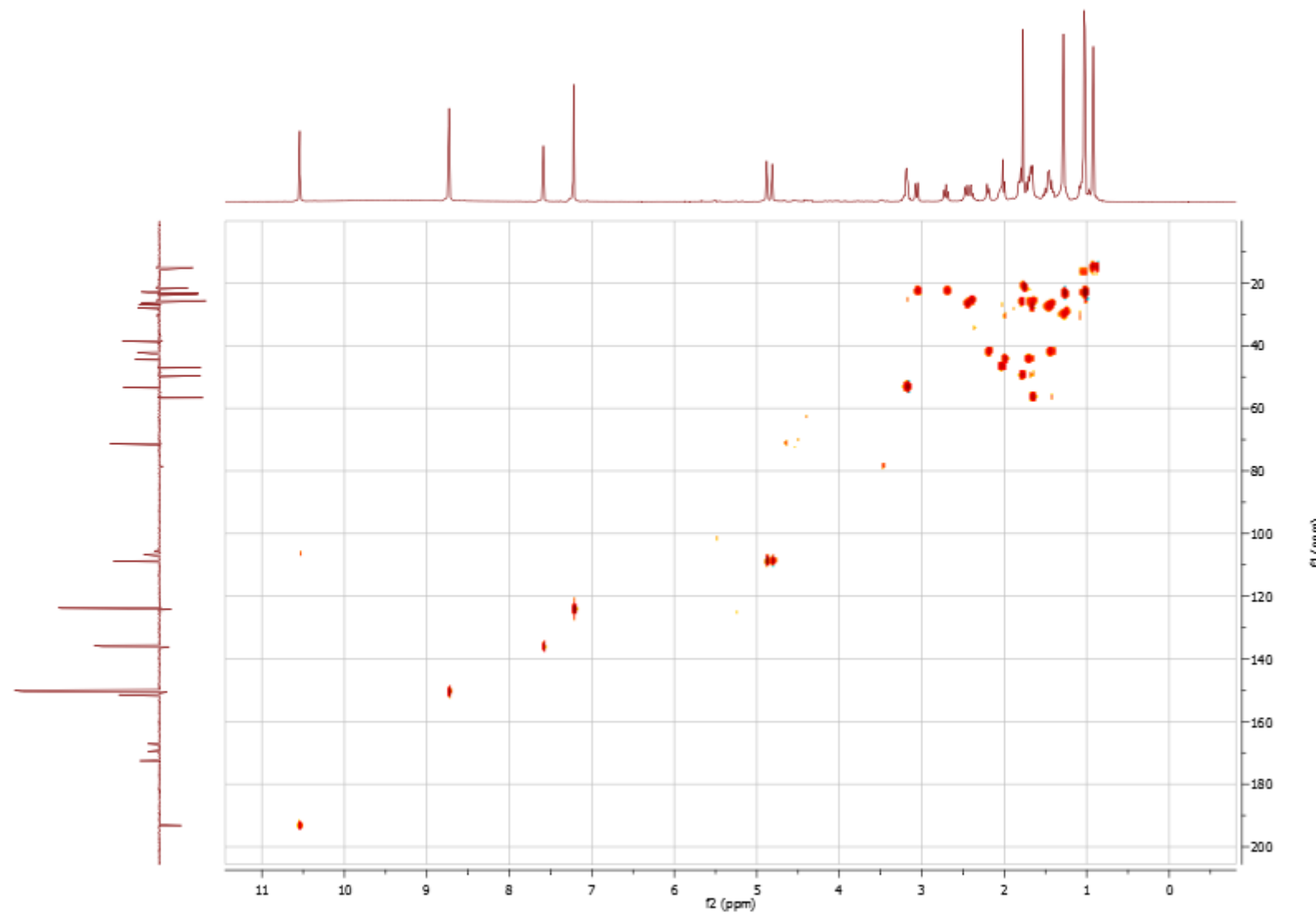
S8. ^1H NMR spectrum of rhodomyrtal A in pyridine- d_5



S9. ^1H - ^1H COSY spectrum of rhodomyrtal A in pyridine- d_5

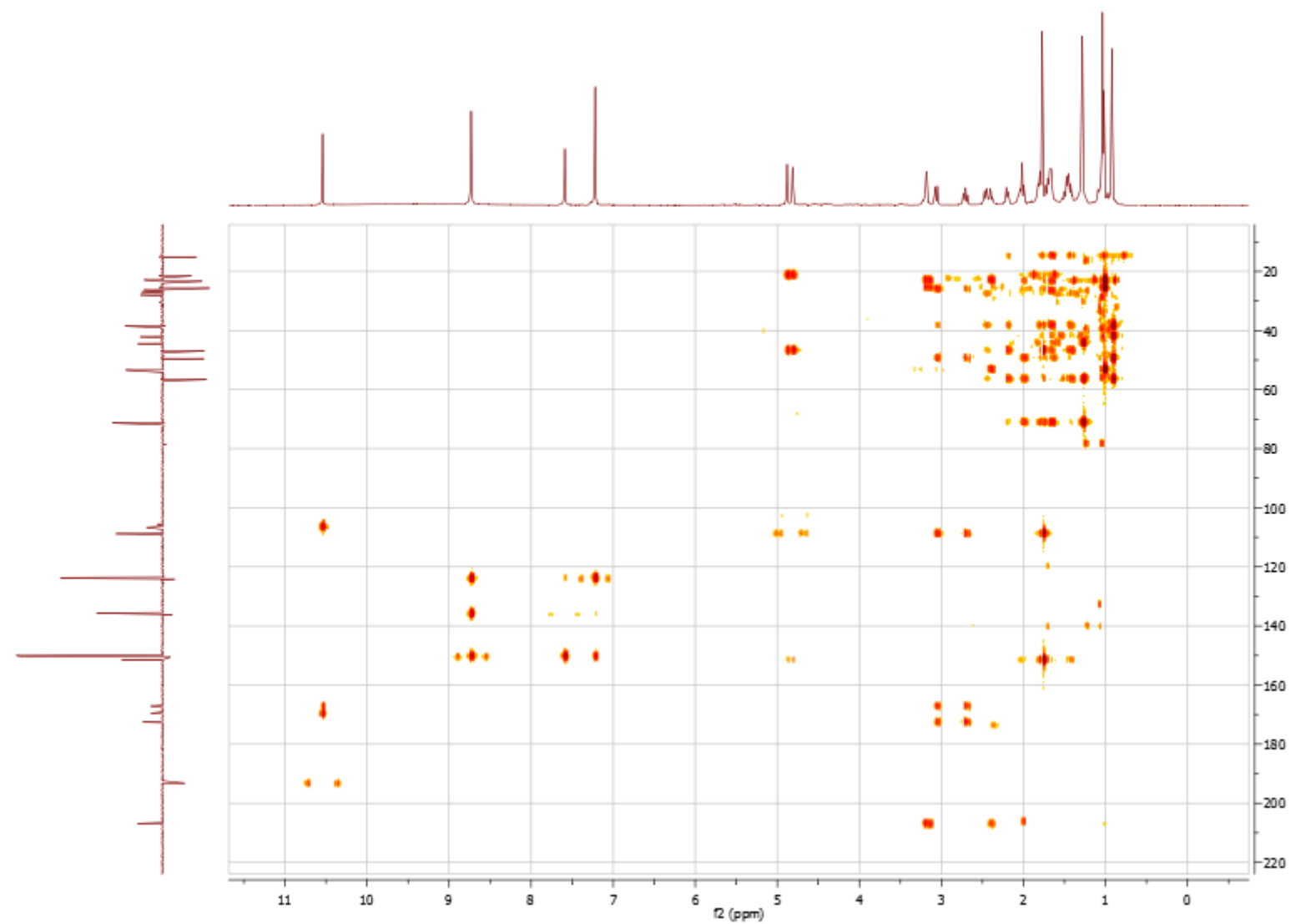


S10. HSQC spectrum of rhodomyrtal A in pyridine-*d*₅



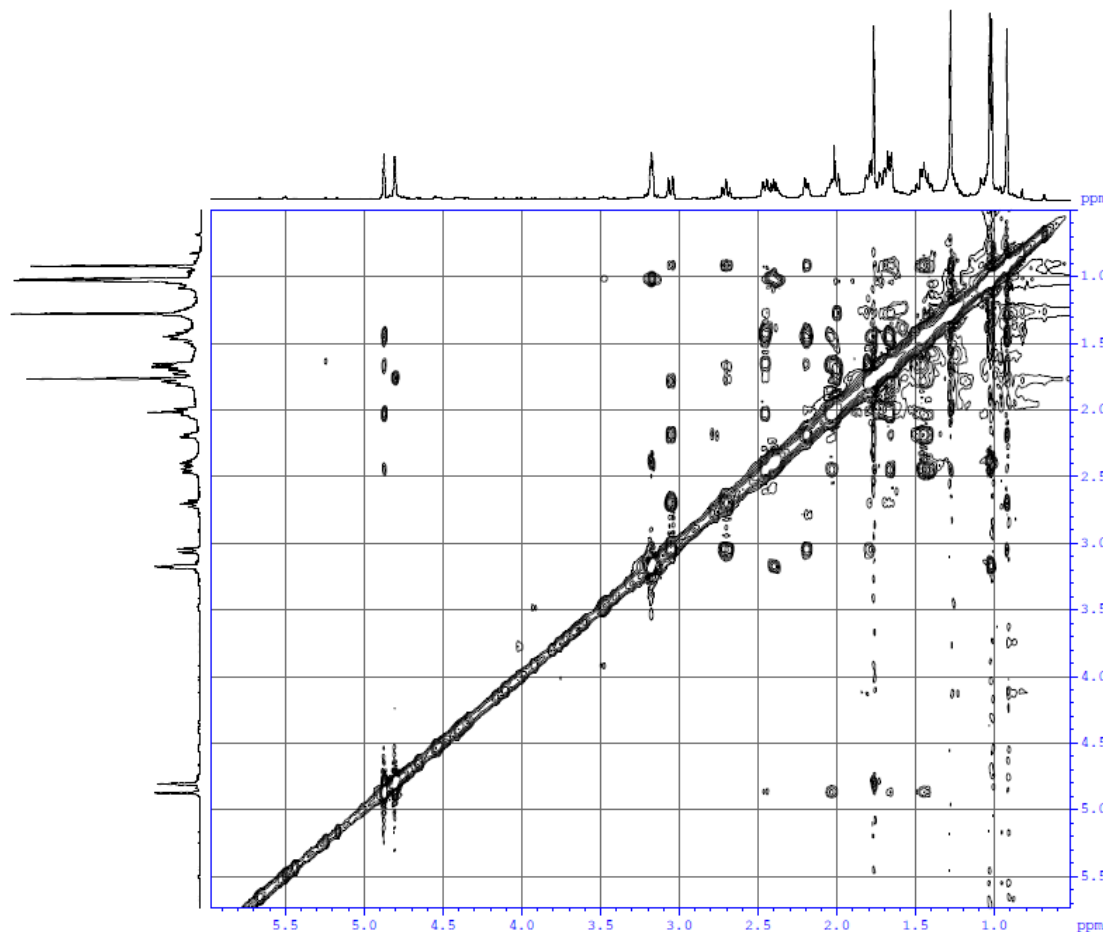
S10

S11. HMBC spectrum of rhodomyrtal A in pyridine-*d*₅



S12. NOESY spectrum of rhodomyrtal A in pyridine-*d*₅

NOESYPHPR



Current Data Parameters
NAME 2012-07-16
EXPNO 2
PROCNO 1

F2 - Acquisition Parameters
Data_ 20120716
Time 13.48
INSTRUM spect
PROBID 5 mm QNP 1H/1
PULPROG noesyphpr
TD 2048
SOLVENT D2O
NS 16
DS 4
SWH 7374.631 Hz
FIDRES 3.600894 Hz
AQ 0.1389044 sec
RG 35.9
DW 67.800 usec
DE 6.00 usec
TE 302.0 K
d0 0.00005857 sec
D1 2.0000000 sec
D2 0.60000002 sec
d11 0.03000000 sec
d12 0.00002000 sec
d13 0.00000400 sec
INO 0.00013560 sec
ST1CNT 128

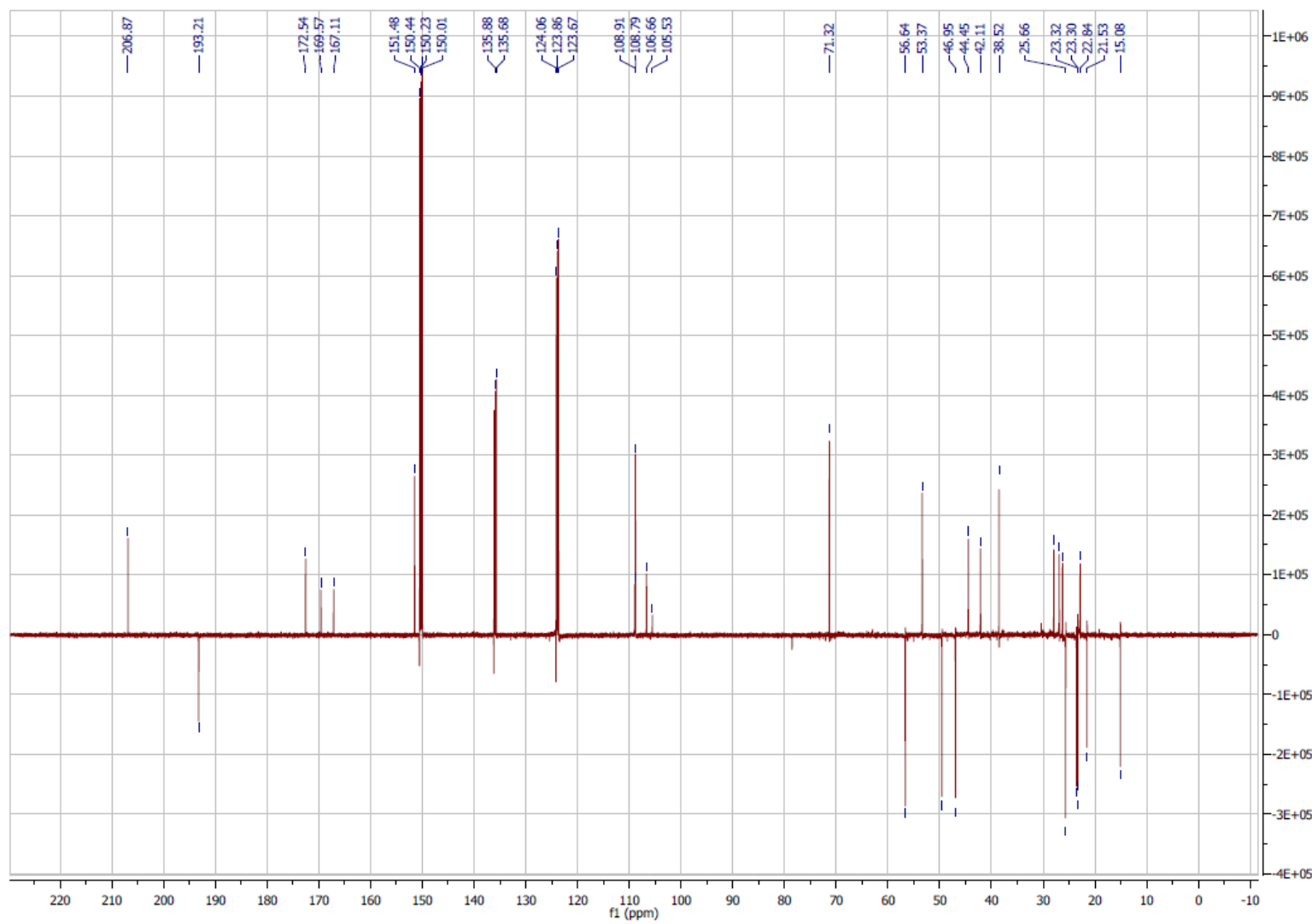
CHANNEL f1
NUC1 1H
P1 7.25 usec
PL1 -4.00 dB
PL9 52.77 dB
SF01 500.1333880 MHz

F1 - Acquisition parameters
NDO 1
TD 256
SF01 500.1334 MHz
FIDRES 28.807144 Hz
SW 14.745 ppm
FnMODE States-TPPI

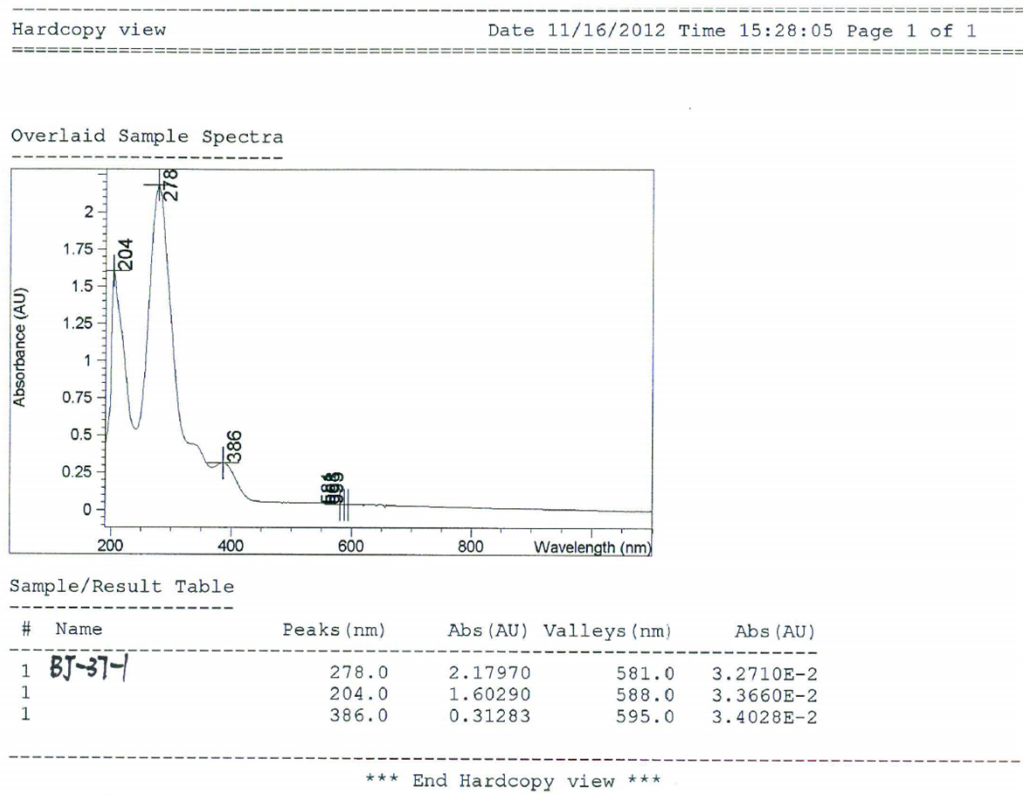
F2 - Processing parameters
SI 2048
SF 500.1299902 MHz
WDW QSINE
SSB 2
LB 0.00 Hz
GB 0
PC 1.00

F1 - Processing parameters
SI 1024
MC2 States-TPPI
SF 500.1299902 MHz
WDW QSINE
SSB 2
LB 0.00 Hz
GB 0

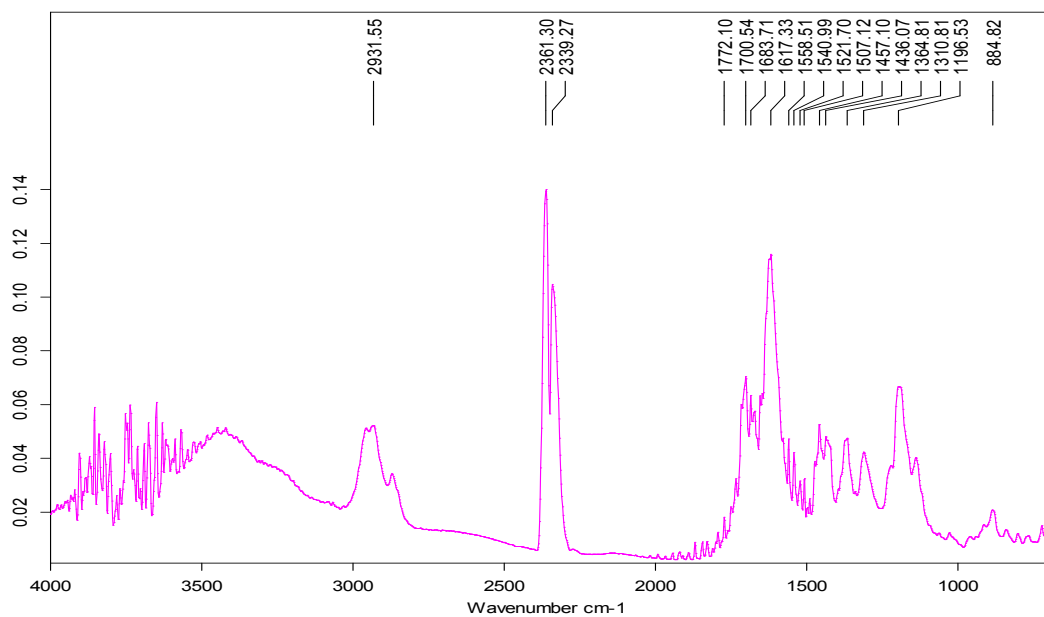
S13. ^{13}C JMORD spectrum of rhodomyrtal A in pyridine- d_5



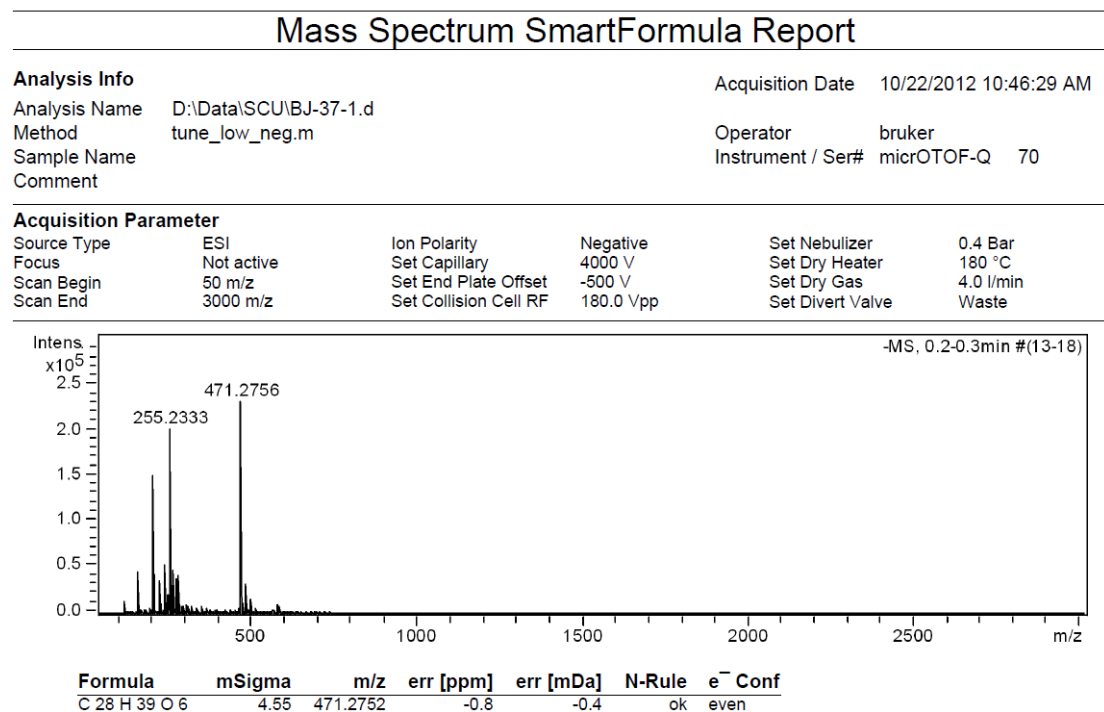
S14. UV spectrum for rhodomyrtal B in methanol



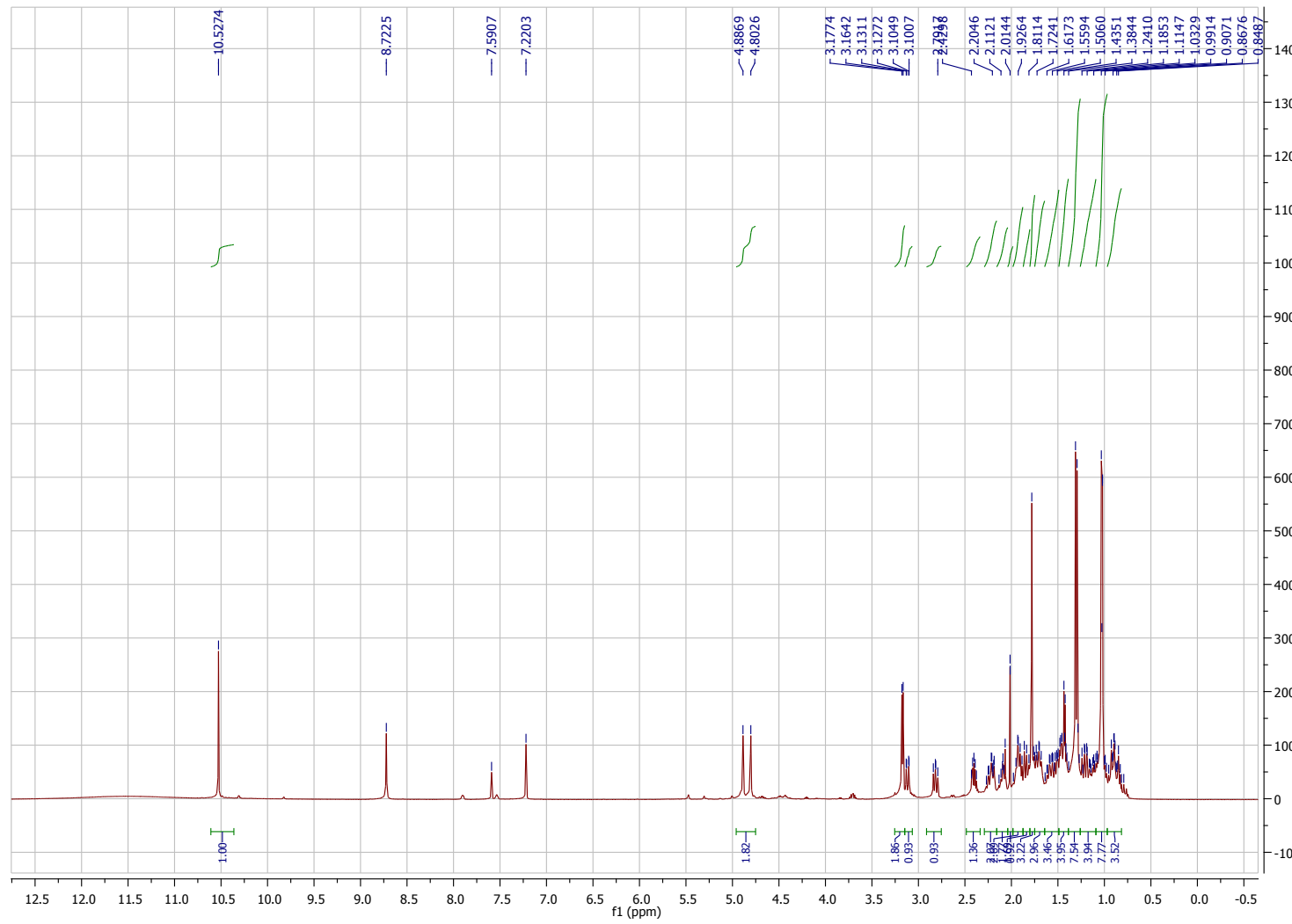
S14. IR spectrum for rhodomyrtal B



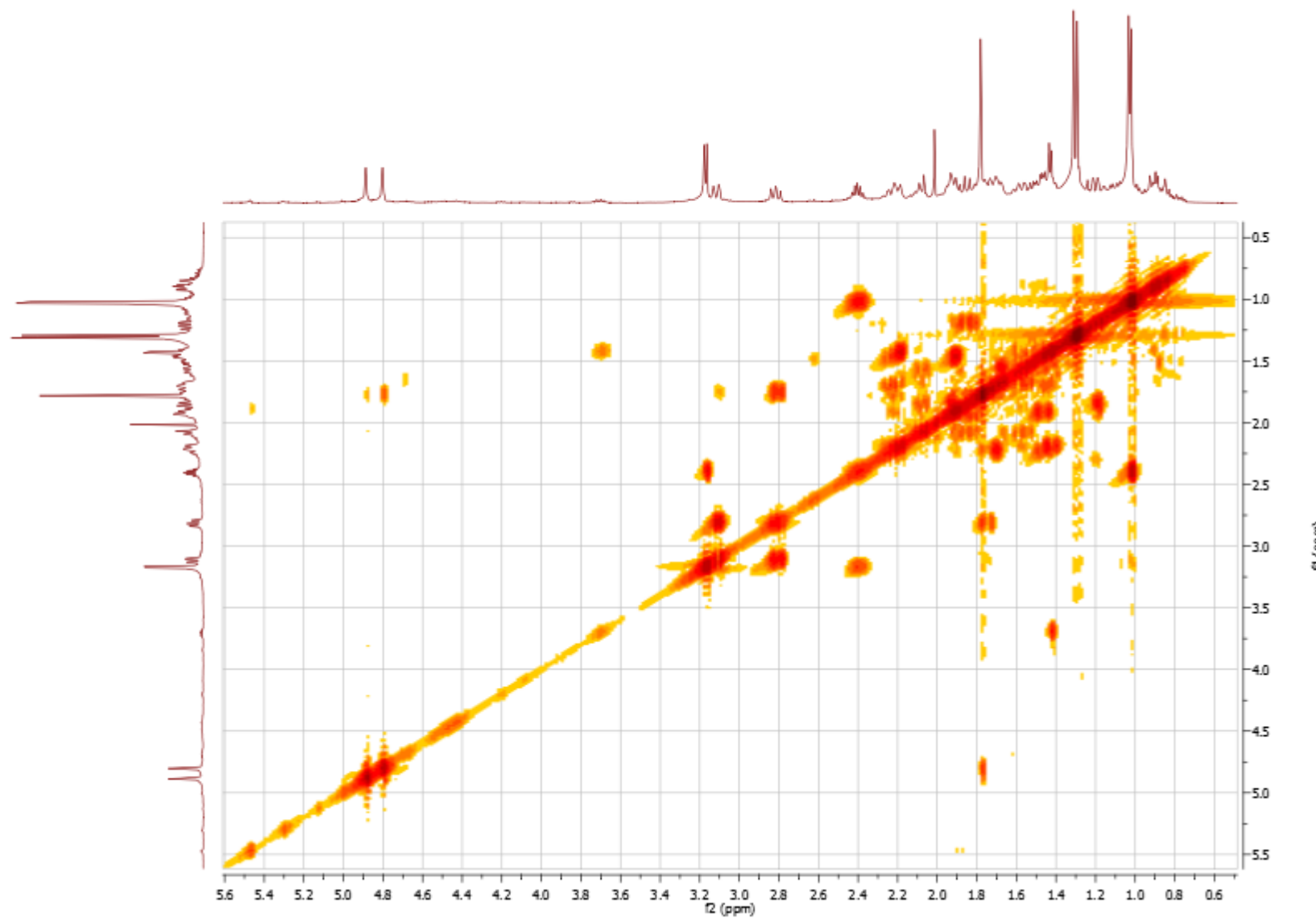
S15. HR-ESI Mass spectrum (negative) of rhodomyrtal B



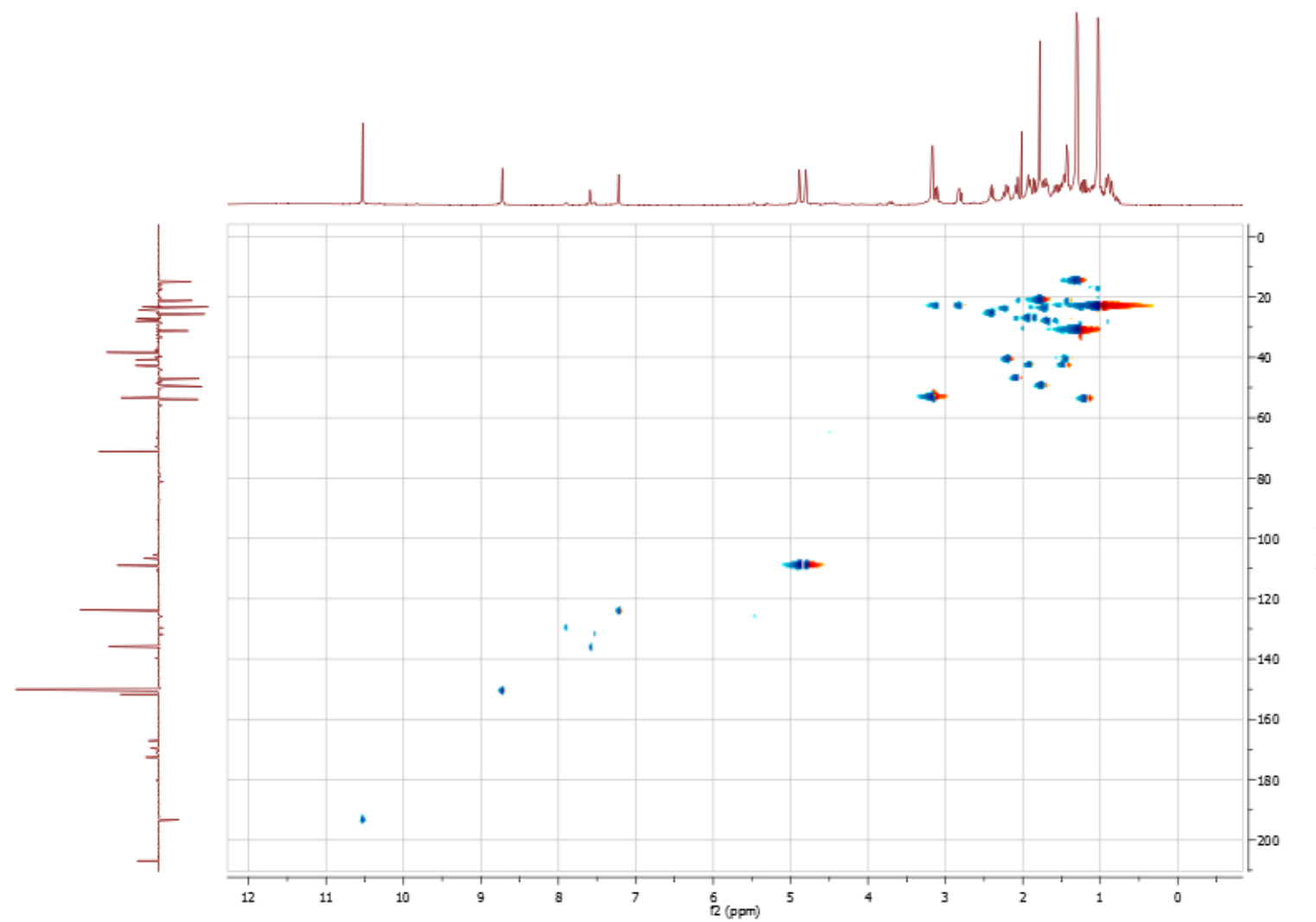
S16. ^1H NMR spectrum of rhodomyrtal B in pyridine- d_5



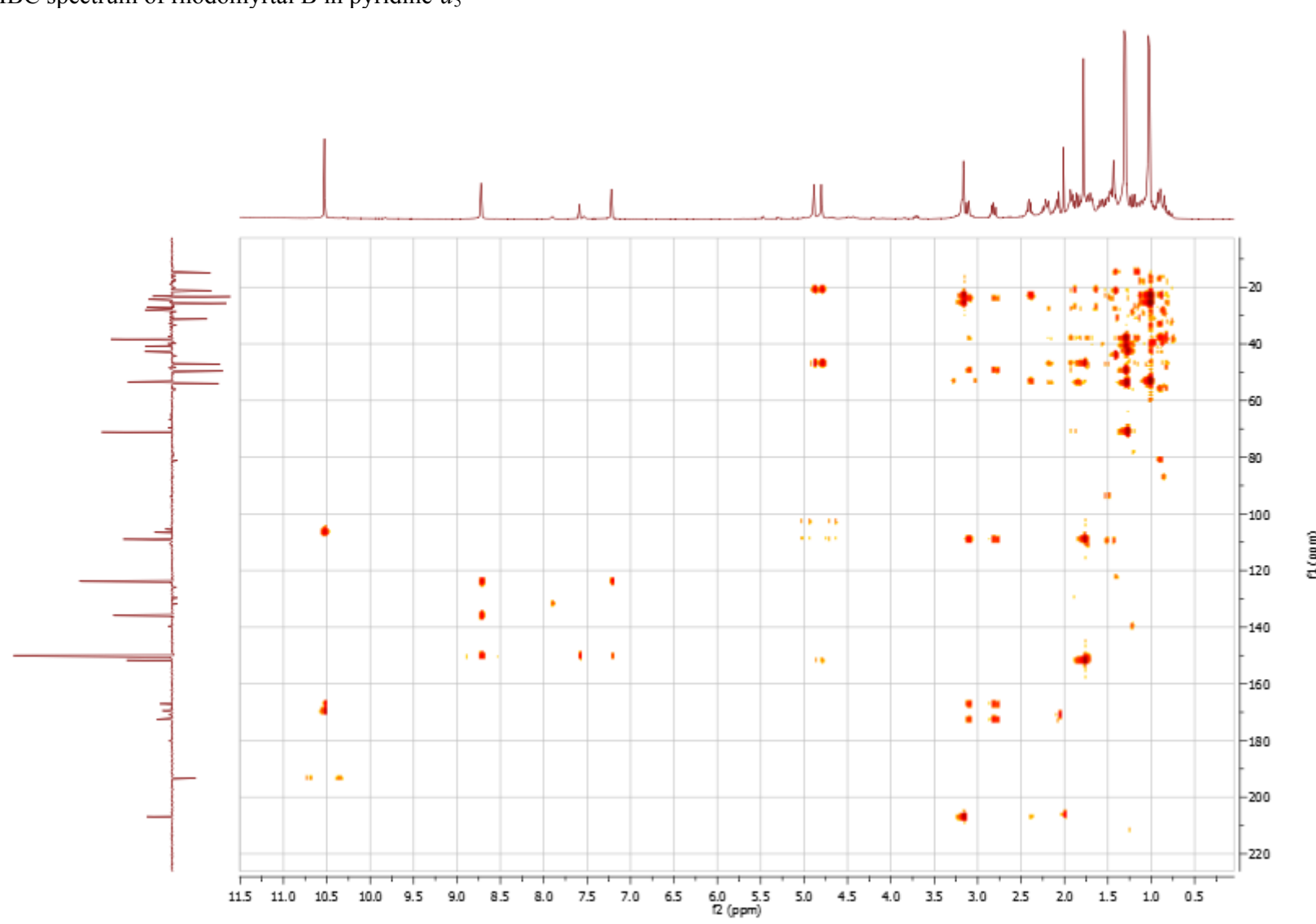
S17. ^1H - ^1H COSY spectrum of rhodomyrtal B in pyridine- d_5



S18. HSQC spectrum of rhodomyrtal B in pyridine-*d*₅

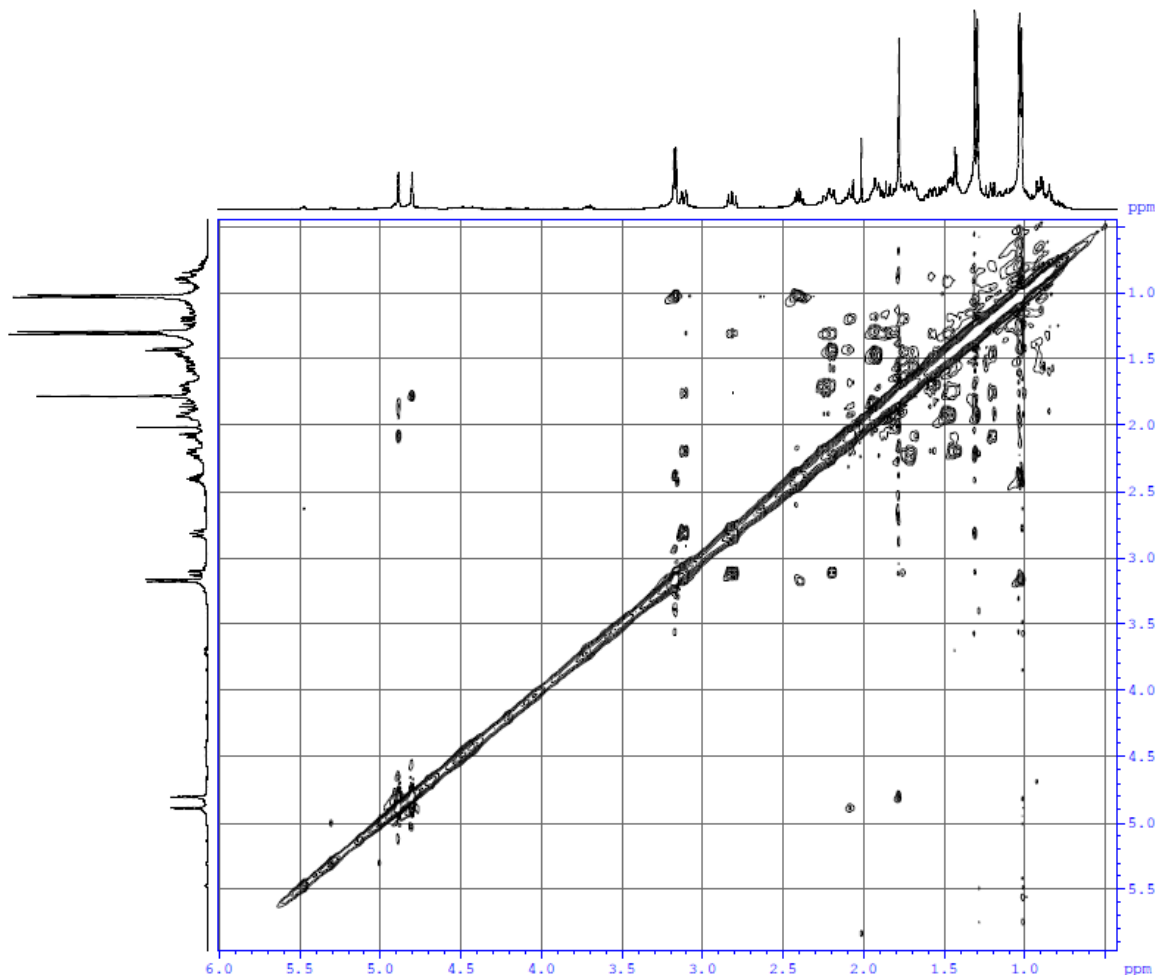


S19. HMBC spectrum of rhodomyrtal B in pyridine-*d*₅



S20. NOESY spectrum of rhodomyrtal B in pyridine-*d*₅

NOESYPHPR



Current Data Parameters
NAME 2012-10-04
EXPNO 1
PROCNO 1

F2 - Acquisition Parameters
Date_ 20121004
Time 11.29
INSTRUM spect
PROBHD 5 mm QNP 1H
PULPROG noesyphpr
TD 2048
SOLVENT D2O
NS 32
DS 4
SWH 6250.000 Hz
FIDRES 3.051758 Hz
AQ 0.1638900 sec
RG 25.4
DW 80.000 usec
DE 6.00 usec
TE 302.0 K
d0 0.00007077 sec
D1 2.0000000 sec
D2 0.6000002 sec
d11 0.03000000 sec
d12 0.0000200 sec
d13 0.00000400 sec
INO 0.0001600 sec
ST1CNT 128

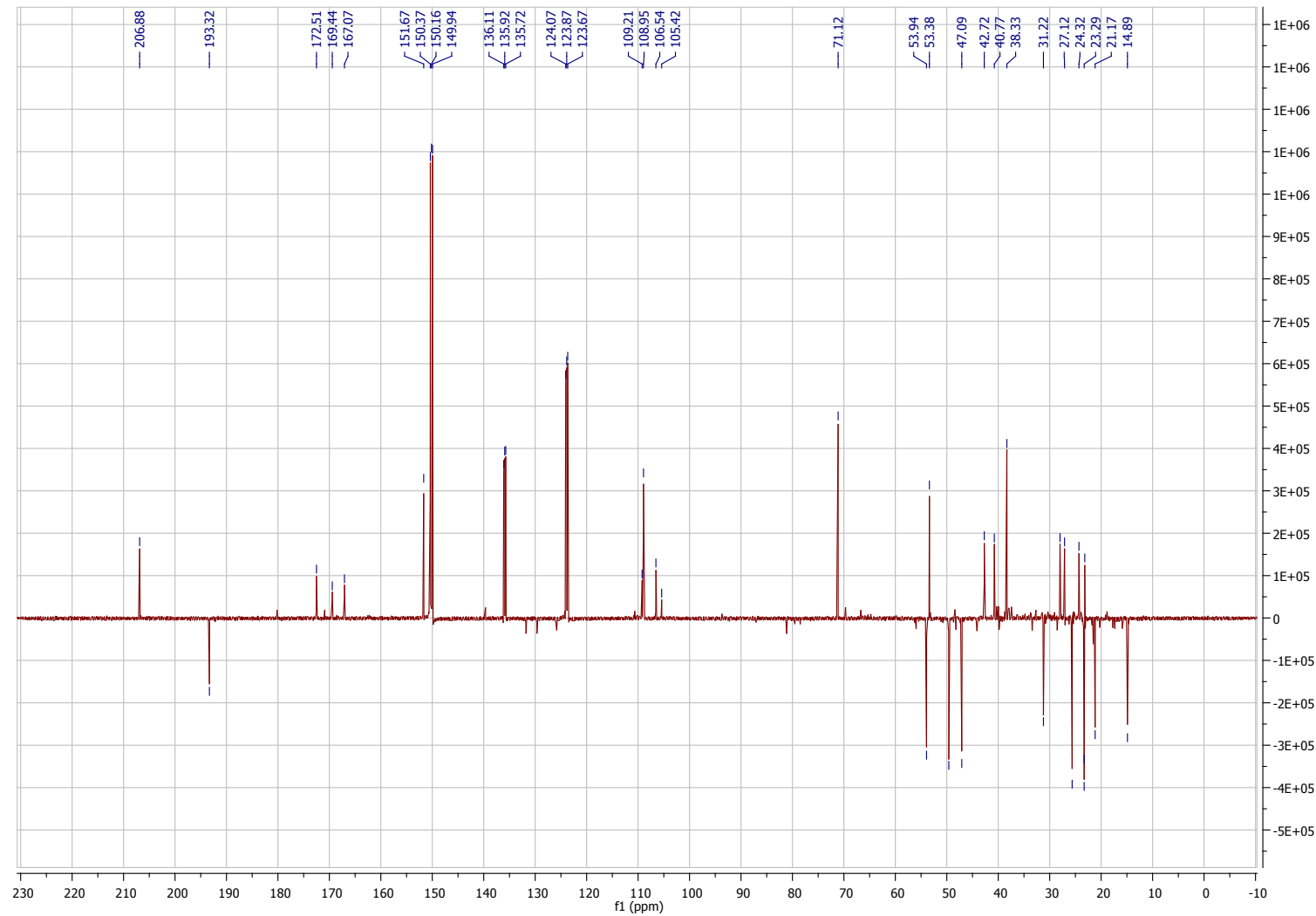
----- CHANNEL f1 -----
NUC1 1H
P1 7.25 usec
PL1 -4.00 dB
PL9 52.77 dB
SFO1 500.1329006 MHz

F1 - Acquisition parameters
ND0 1
TD 256
SFO1 500.1329 MHz
FIDRES 24.414063 Hz
SW 12.497 ppm
FnMODE States-TPPI

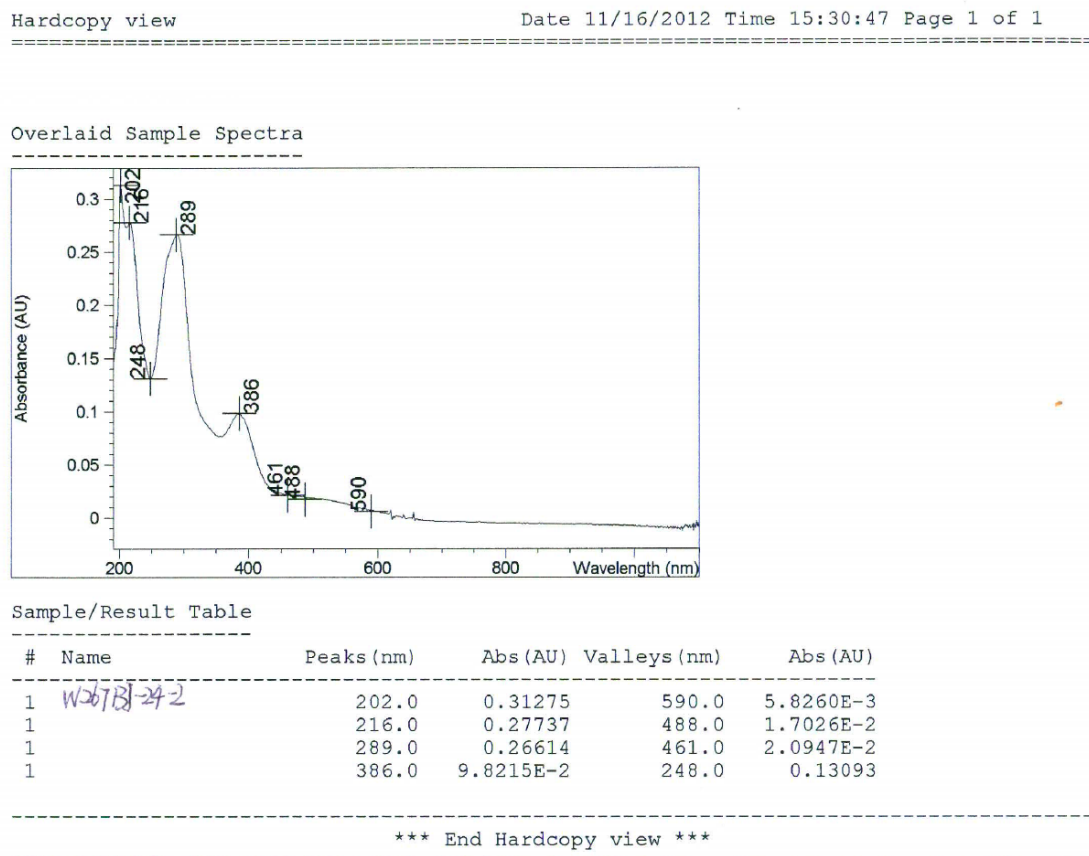
F2 - Processing parameters
SI 2048
SF 500.1299909 MHz
WDW QSINE
SSB 2
LB 0.00 Hz
GB 0
PC 1.00

F1 - Processing parameters
SI 1024
MC2 States-TPPI
SF 500.1299909 MHz
WDW QSINE
SSB 2
LB 0.00 Hz
GB 0

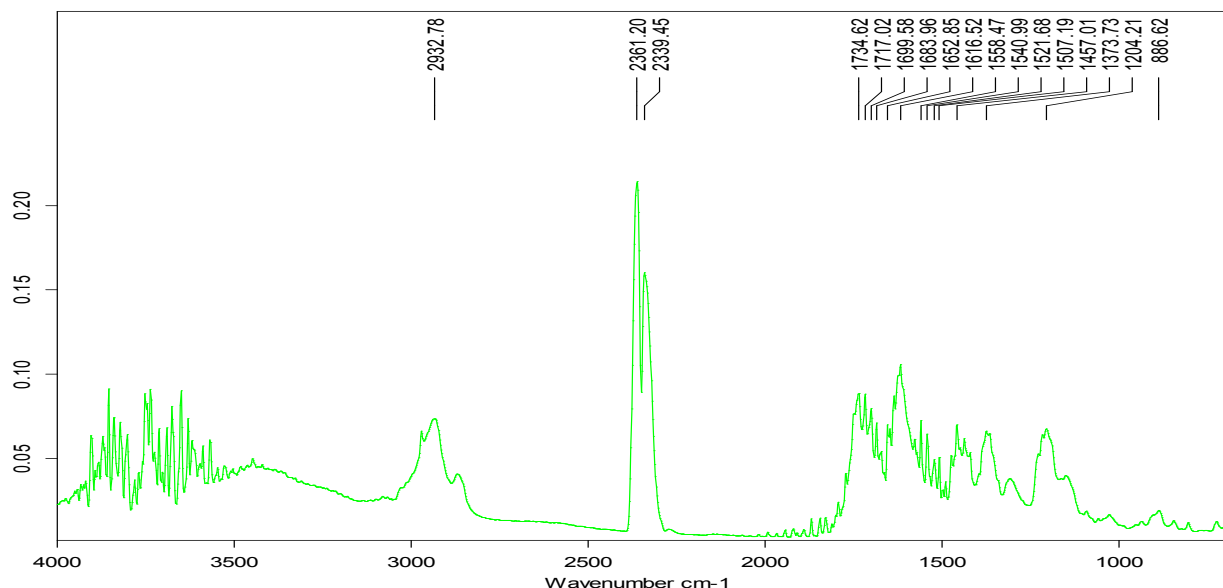
S21. ^{13}C JMOD spectrum of rhodomyrtal B in pyridine- d_5



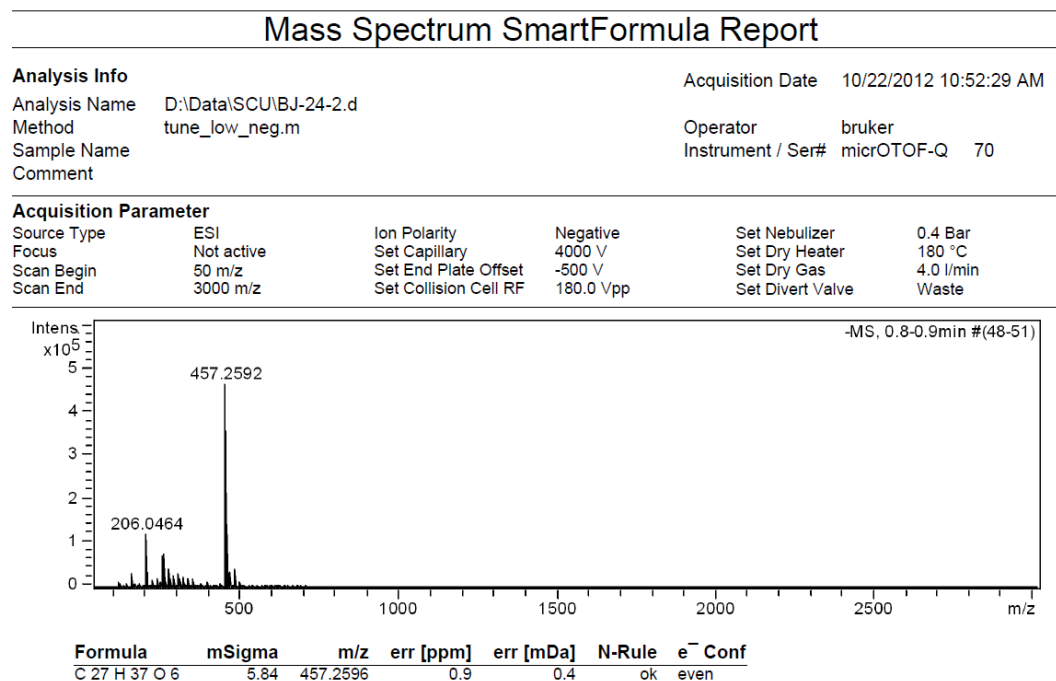
S22. UV spectrum for rhodomyrtal C in methanol



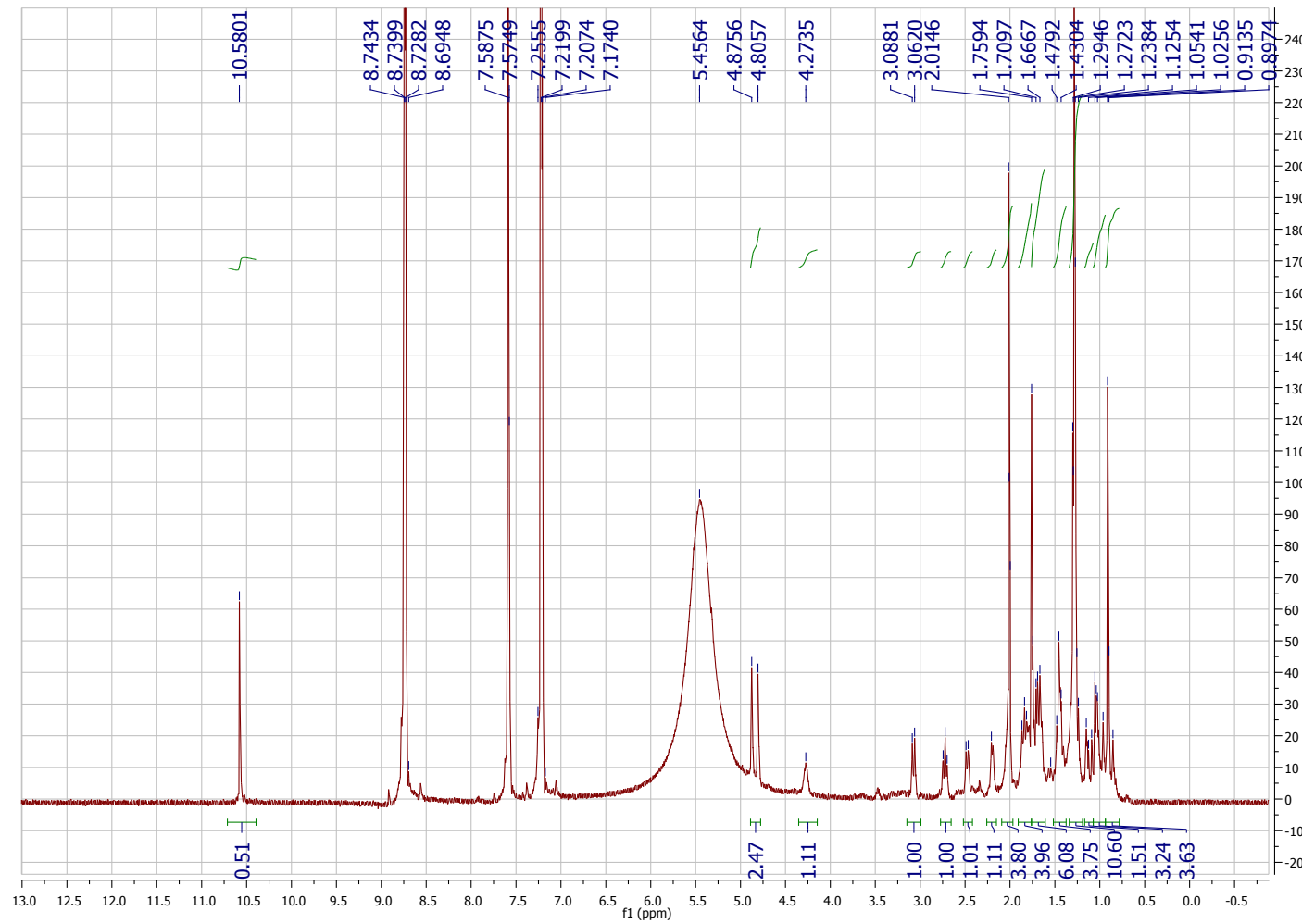
S22. IR spectrum for rhodomyrtal C



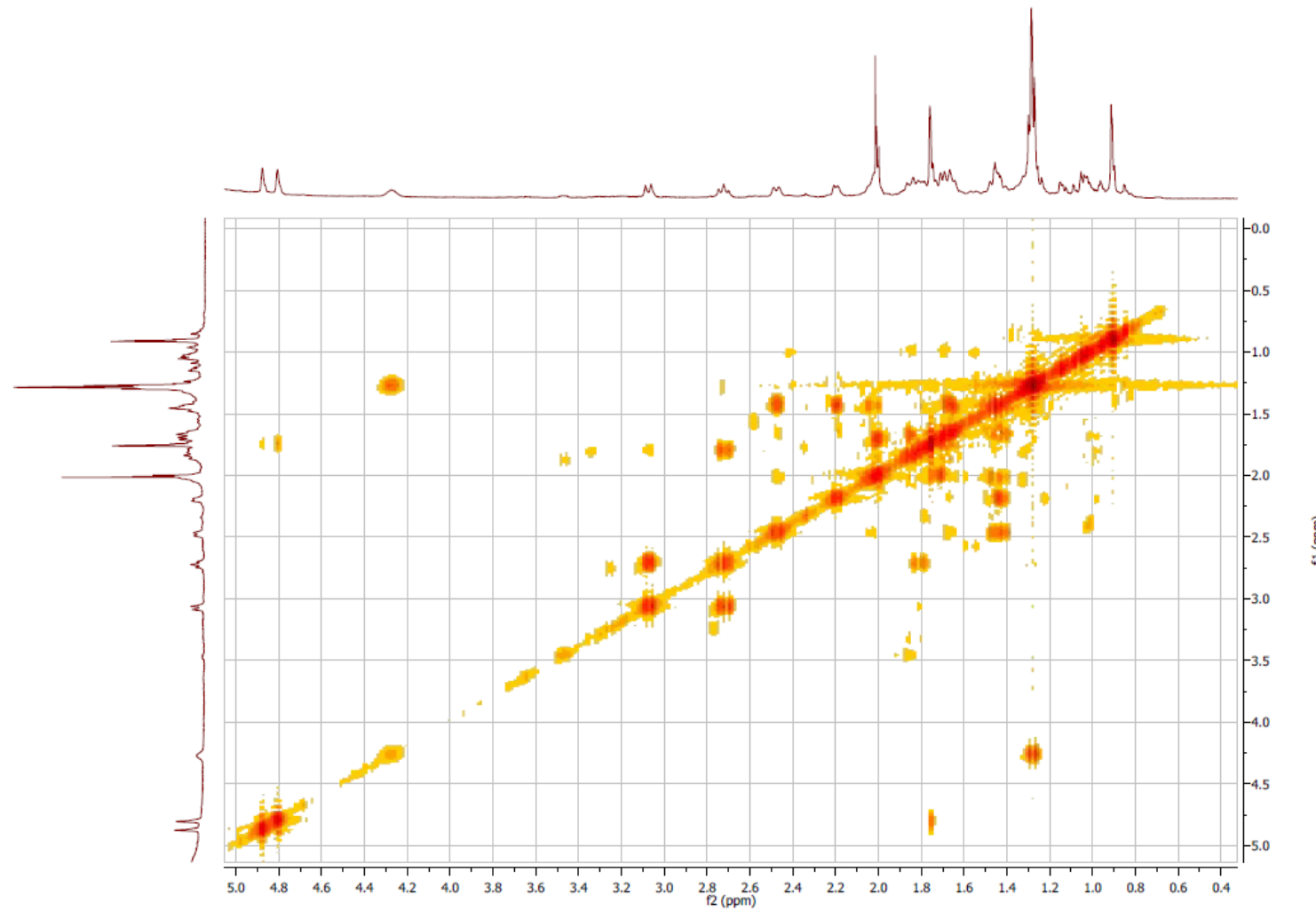
S23. HR-ESI Mass spectrum (negative) of rhodomyrtal C



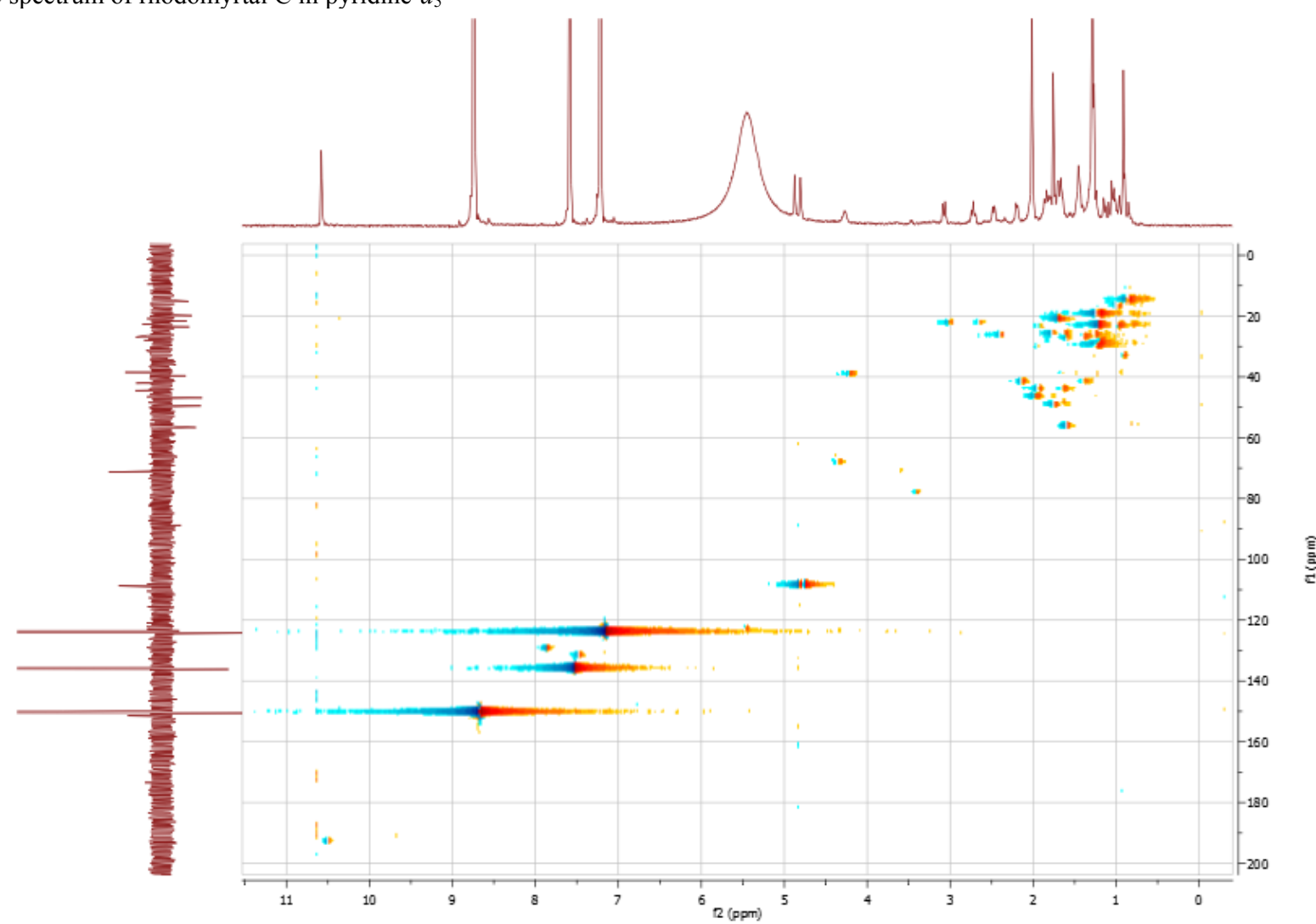
S24. ^1H NMR spectrum of rhodomyrtal C in pyridine- d_5



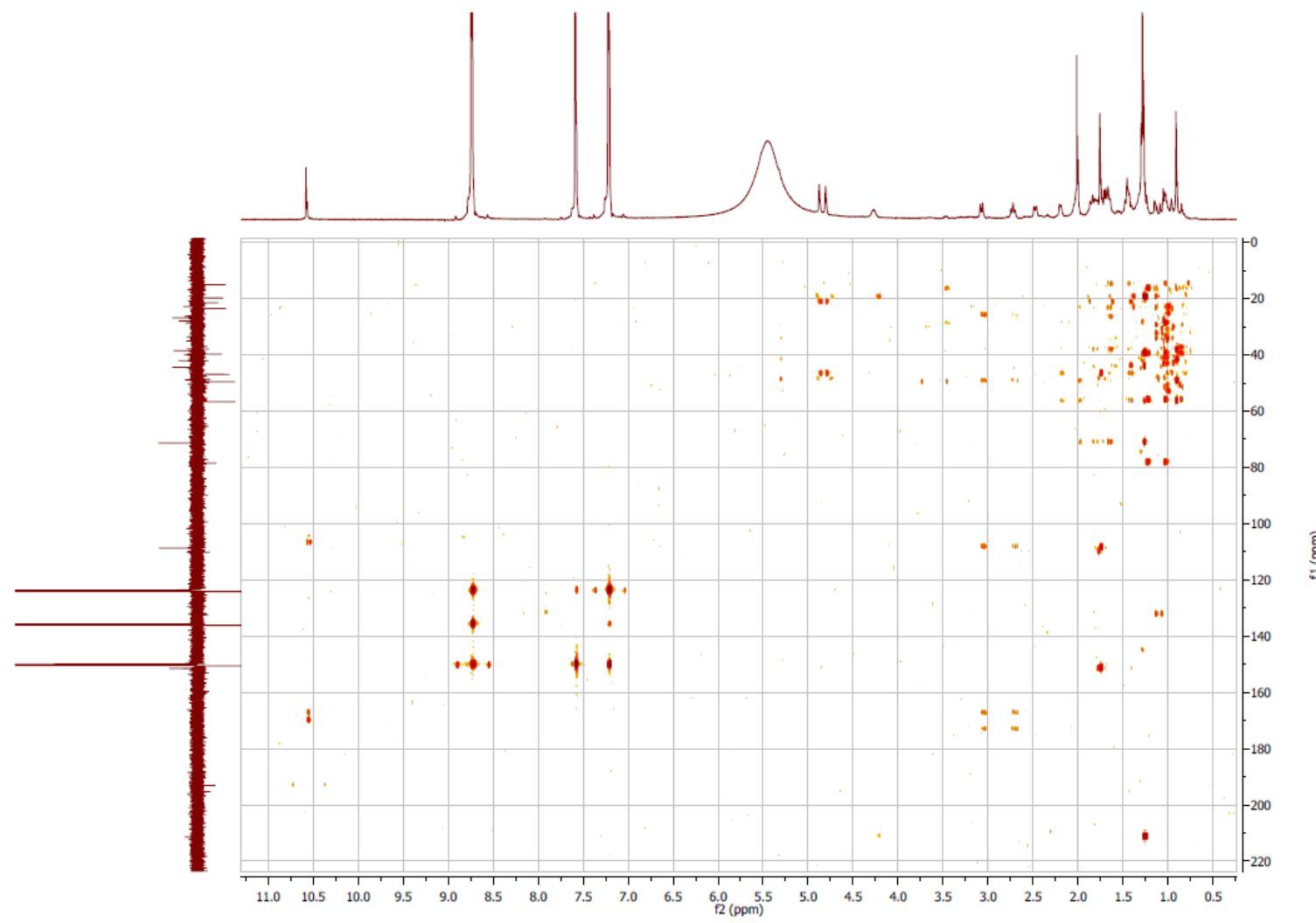
S25. ^1H - ^1H COSY spectrum of rhodomyrtal C in pyridine- d_5



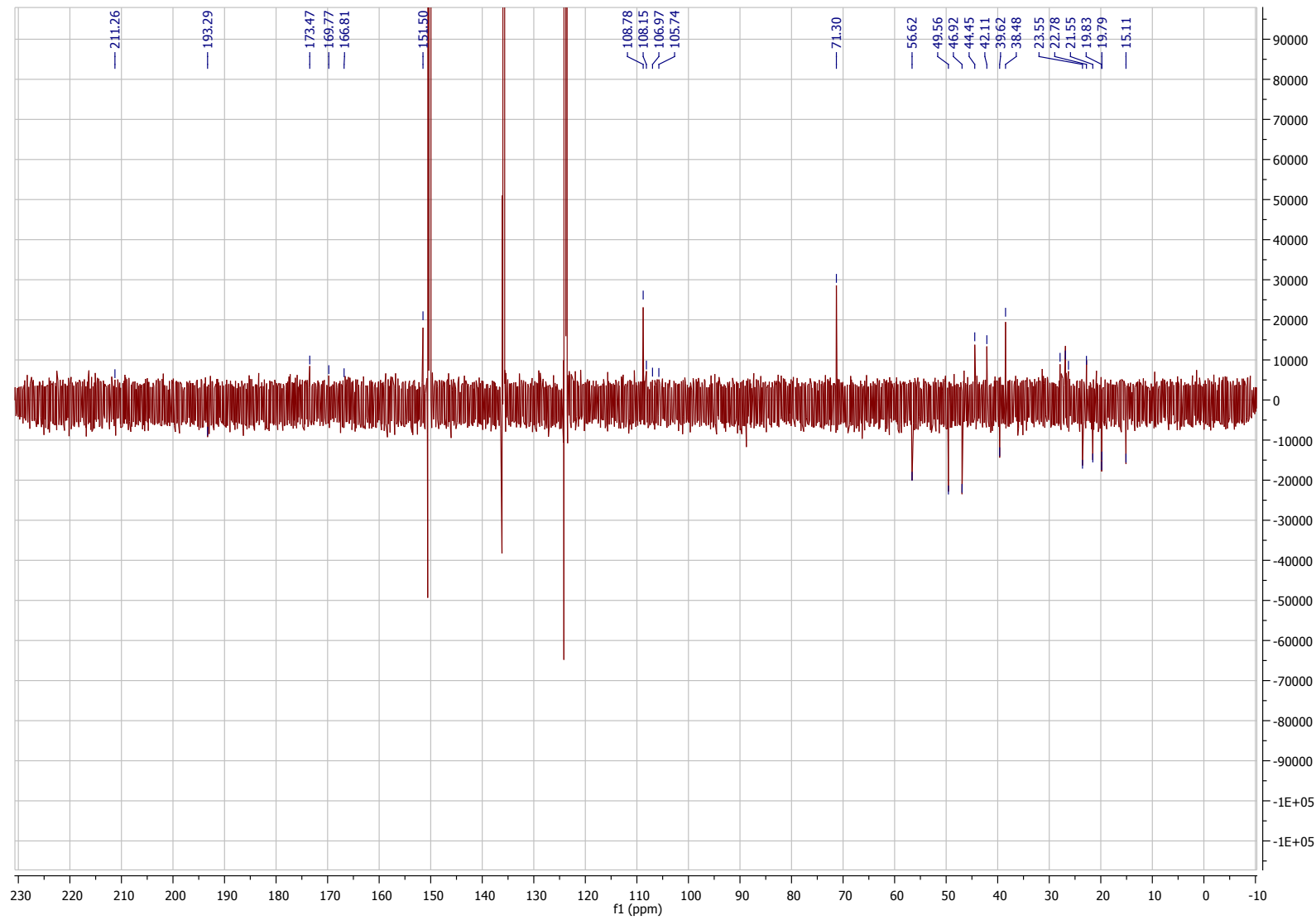
S26. HSQC spectrum of rhodomyrtal C in pyridine-*d*₅



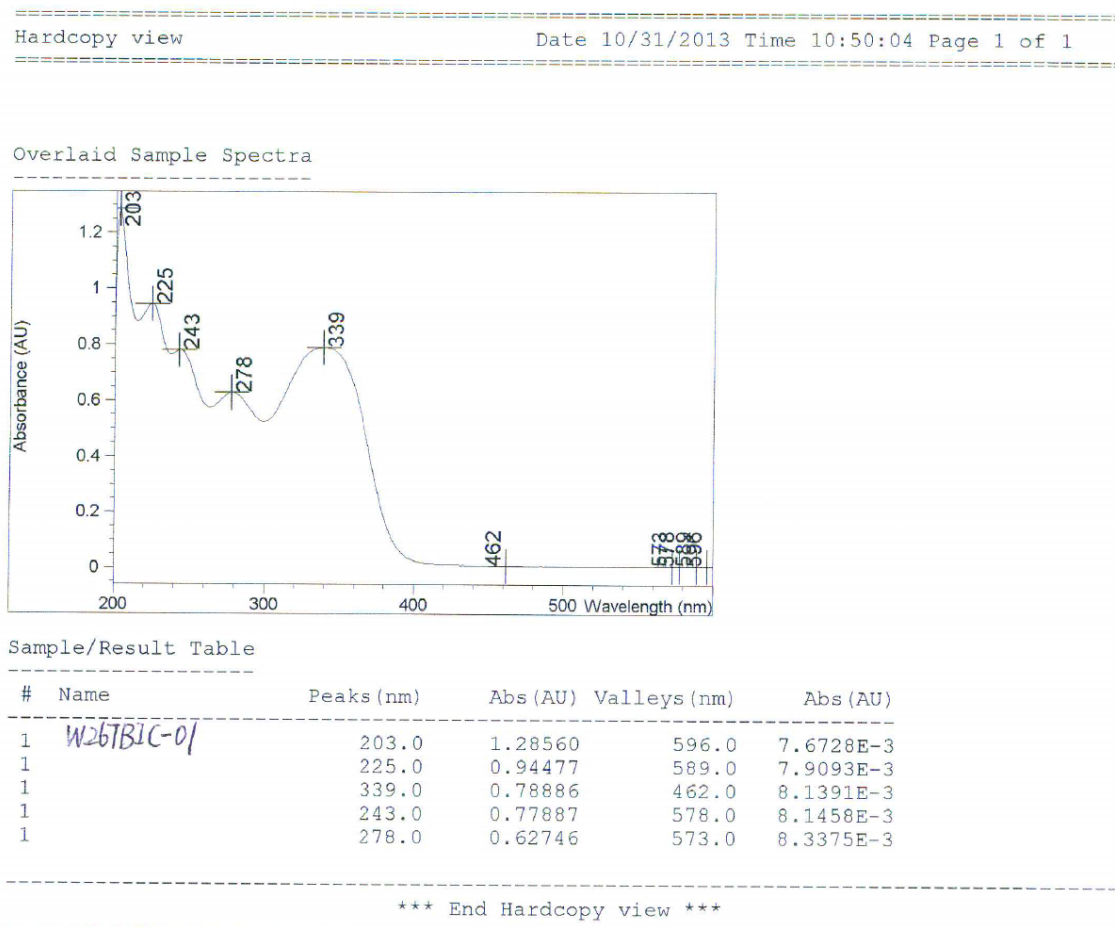
S27. HMBC spectrum of rhodomyrtal C in pyridine-*d*₅



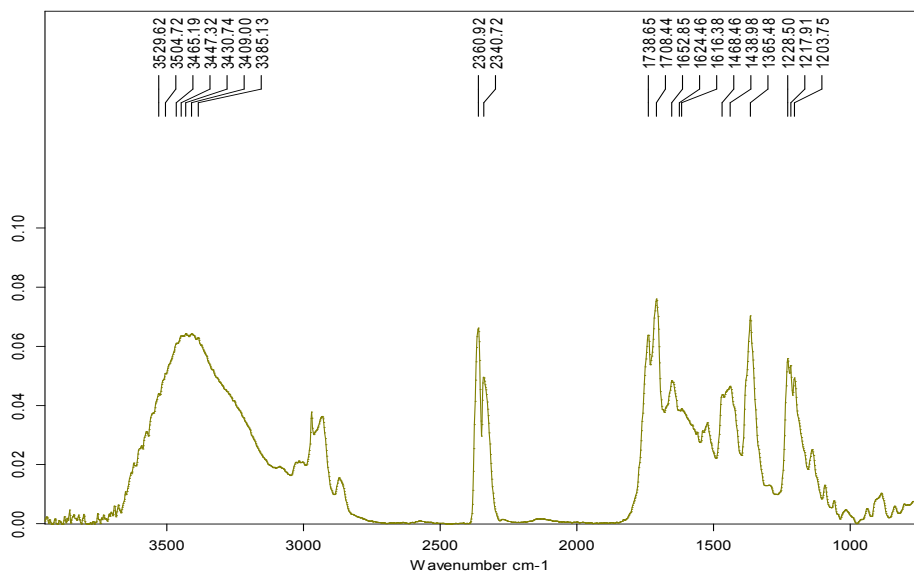
S28. ^{13}C JMOD spectrum of rhodomyrtal C in pyridine- d_5



S29. UV spectrum for rhodomyrtal D in methanol



S29. IR spectrum for rhodomyrtal D



S30. HR-ESI Mass spectrum (negative) of rhodomyrtal D

Mass Spectrum SmartFormula Report

Analysis Info		Acquisition Date	10/16/2012 2:59:49 PM
Analysis Name	D:\Data\SCU\W267BIC-01neg2.d	Operator	bruker
Method	tune_low_neg.m	Instrument / Ser#	micrOTOF-Q 70
Sample Name			
Comment			

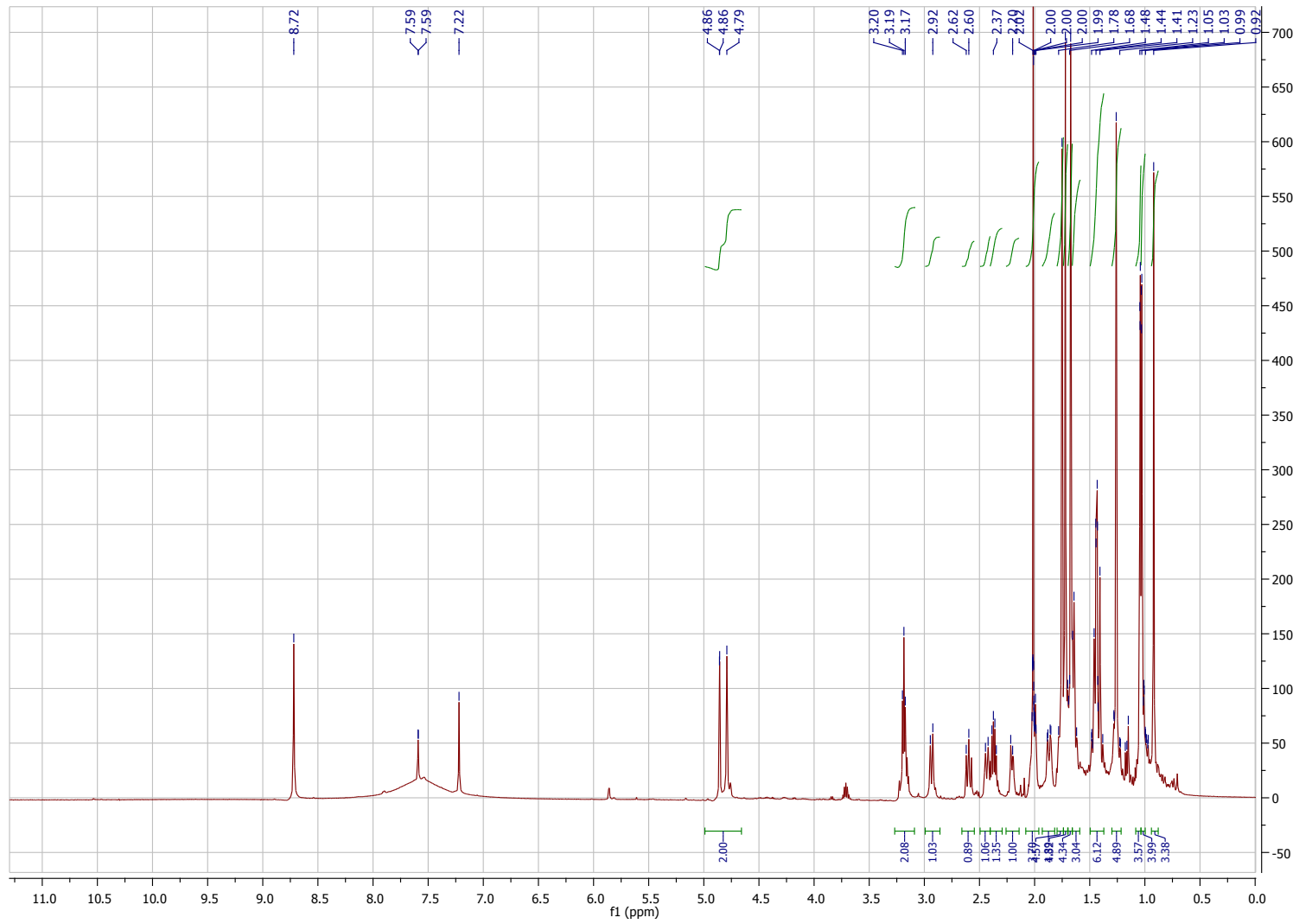
Acquisition Parameter

Source Type	ESI	Ion Polarity	Negative	Set Nebulizer	0.4 Bar
Focus	Not active	Set Capillary	4000 V	Set Dry Heater	180 °C
Scan Begin	50 m/z	Set End Plate Offset	-500 V	Set Dry Gas	4.0 l/min
Scan End	3000 m/z	Set Collision Cell RF	180.0 V _{pp}	Set Divert Valve	Waste



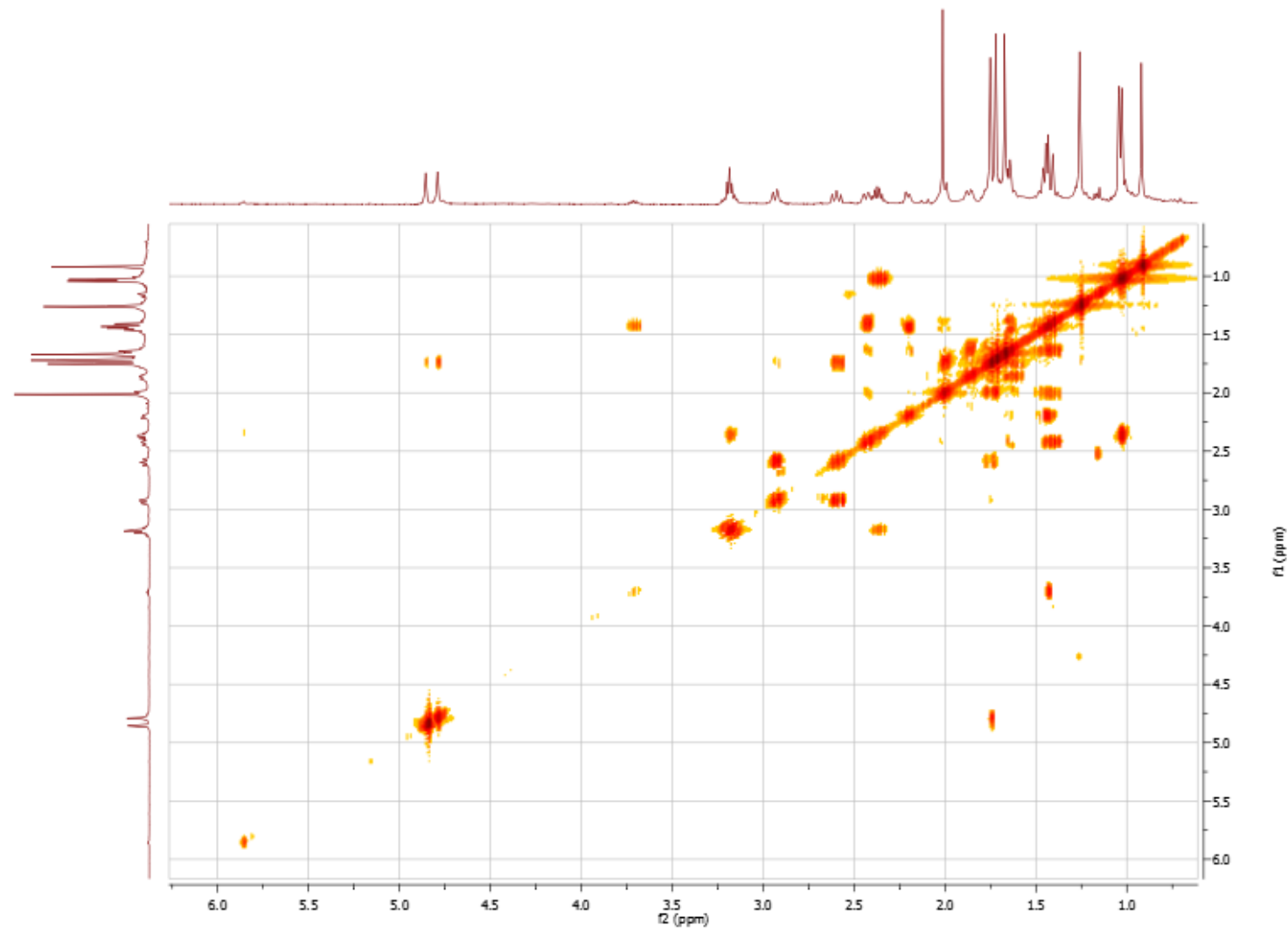
Formula	mSigma	m/z	err [ppm]	err [mDa]	N-Rule	e ⁻ Conf
C ₂₉ H ₄₃ O ₅	43.47	471.3116	2.0	0.9	ok	even

S31. ^1H NMR spectrum of rhodomyrtal D in pyridine- d_5



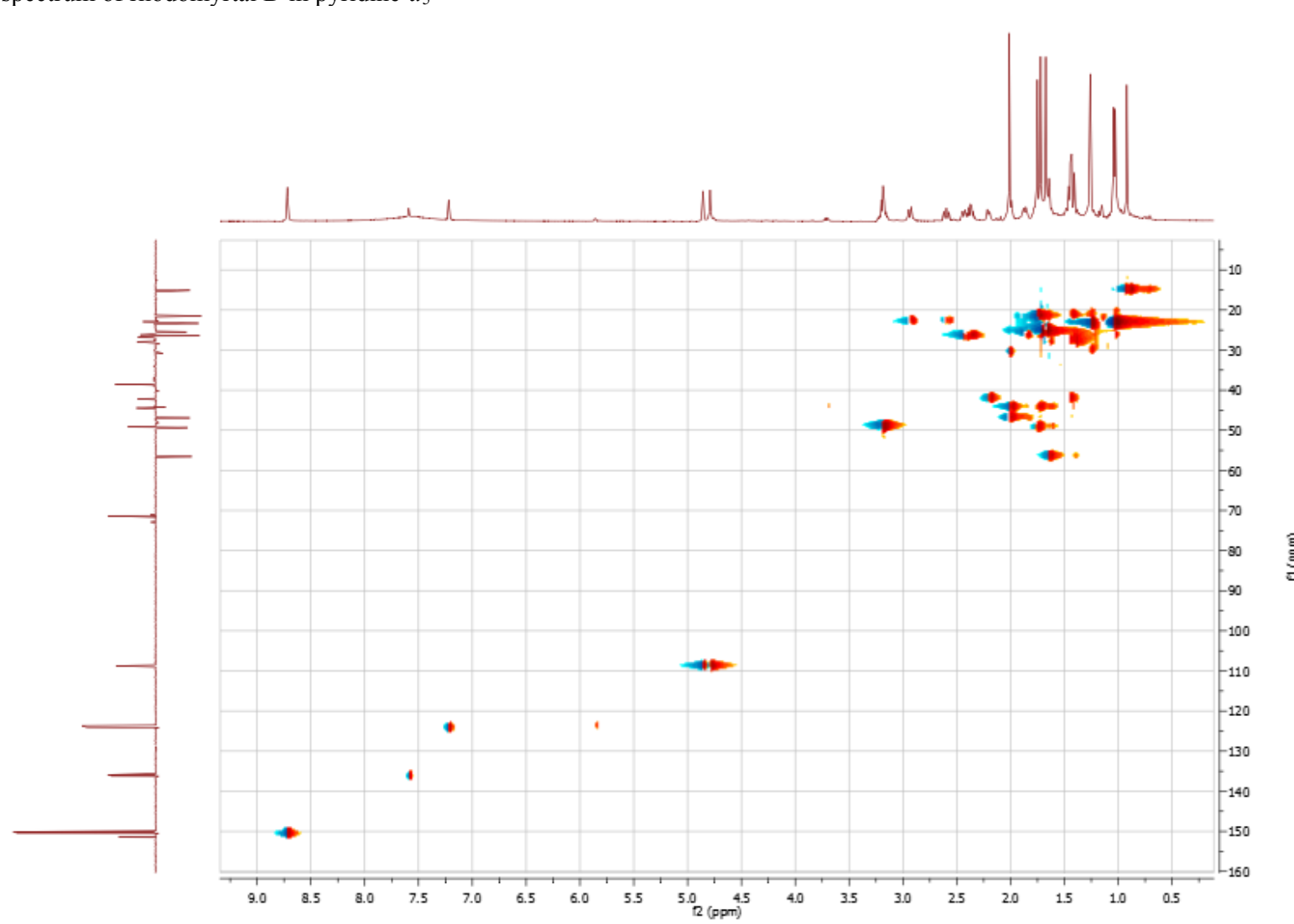
S31

S32. ^1H - ^1H COSY spectrum of rhodomyrtal D in pyridine- d_5



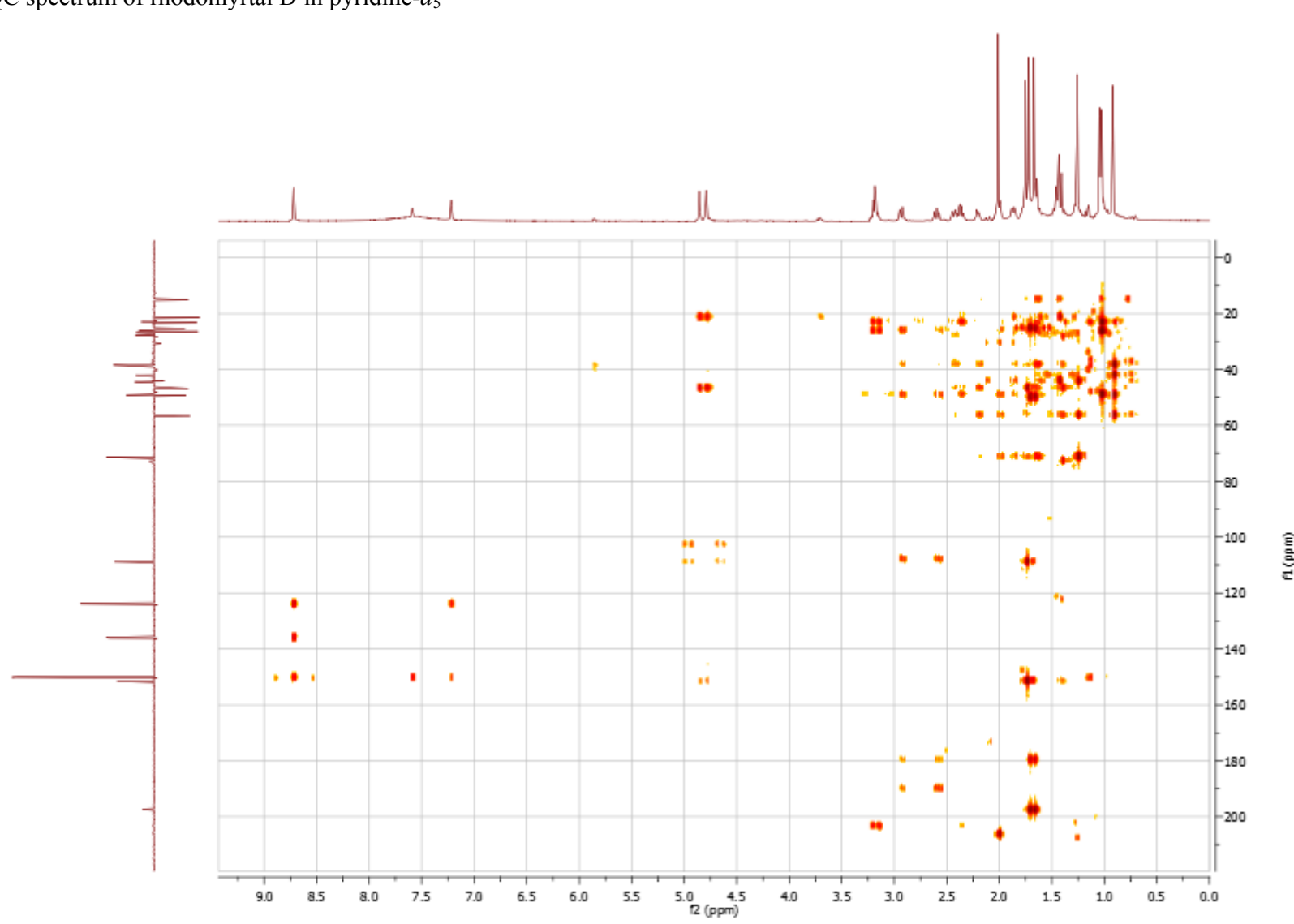
S32

S33. HSQC spectrum of rhodomyrtal D in pyridine-*d*₅



S33

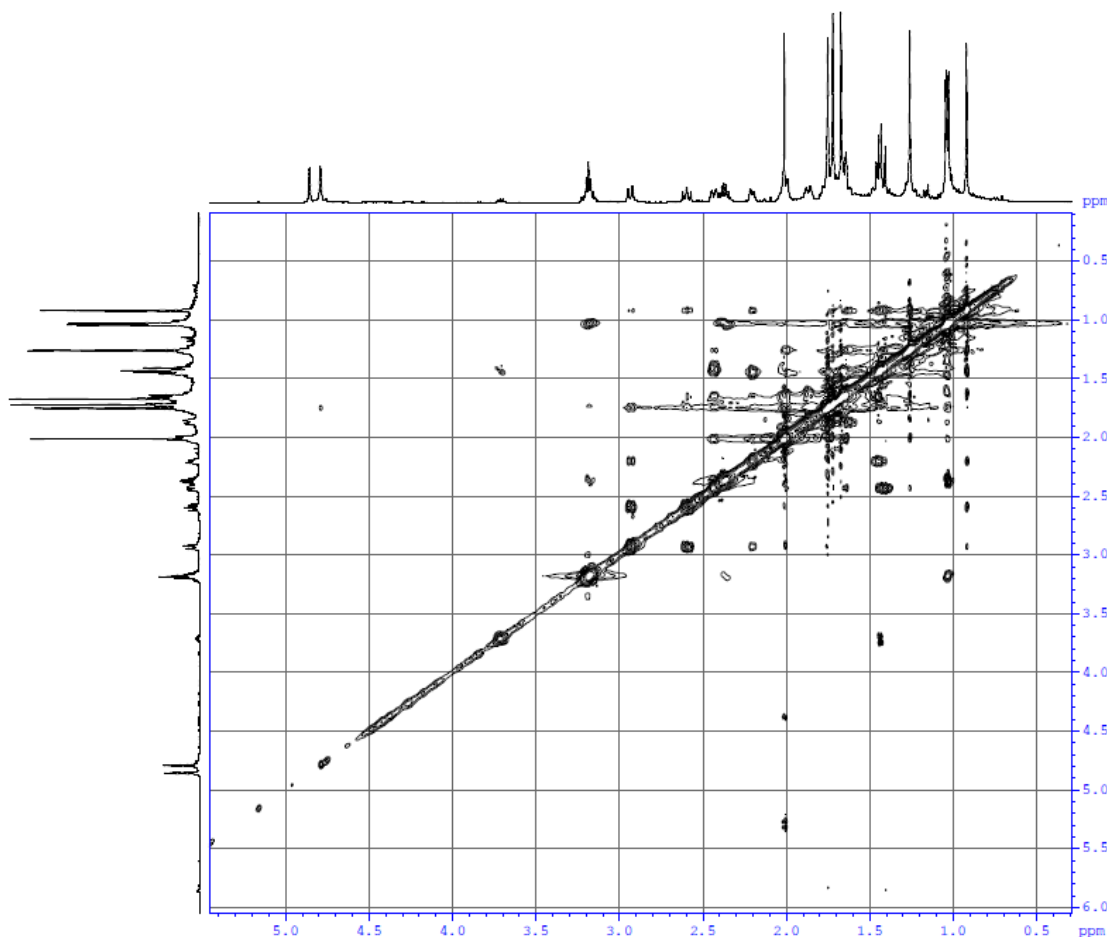
S34. HMQC spectrum of rhodomyrtal D in pyridine-*d*₅



S34

S35. NOESY spectrum of rhodomyrtal D in pyridine-*d*₅

NOESYPHPR



Current Data Parameters
NAME 2012-10-19
EXPNO 6
PROCNO 1

P2 - Acquisition Parameters
Data_ 20121019
Time 19.41
INSTRUM spect
PROBHD 5 mm QNP 1H/1
PULPROG noesyphpr
TD 2048
SOLVENT D2O
NS 32
DS 4
SWH 5208.333 Hz
FIDRES 2.543132 Hz
AQ 0.1966580 sec
RG 25.4
DW 96.000 usec
DE 6.00
TE 300.0 K
d0 0.0000877 sec
D1 2.0000000 sec
D2 0.6000002 sec
d11 0.0300000 sec
d12 0.0000200 sec
d13 0.0000400 sec
INO 0.00019200 sec
ST1CNT 128

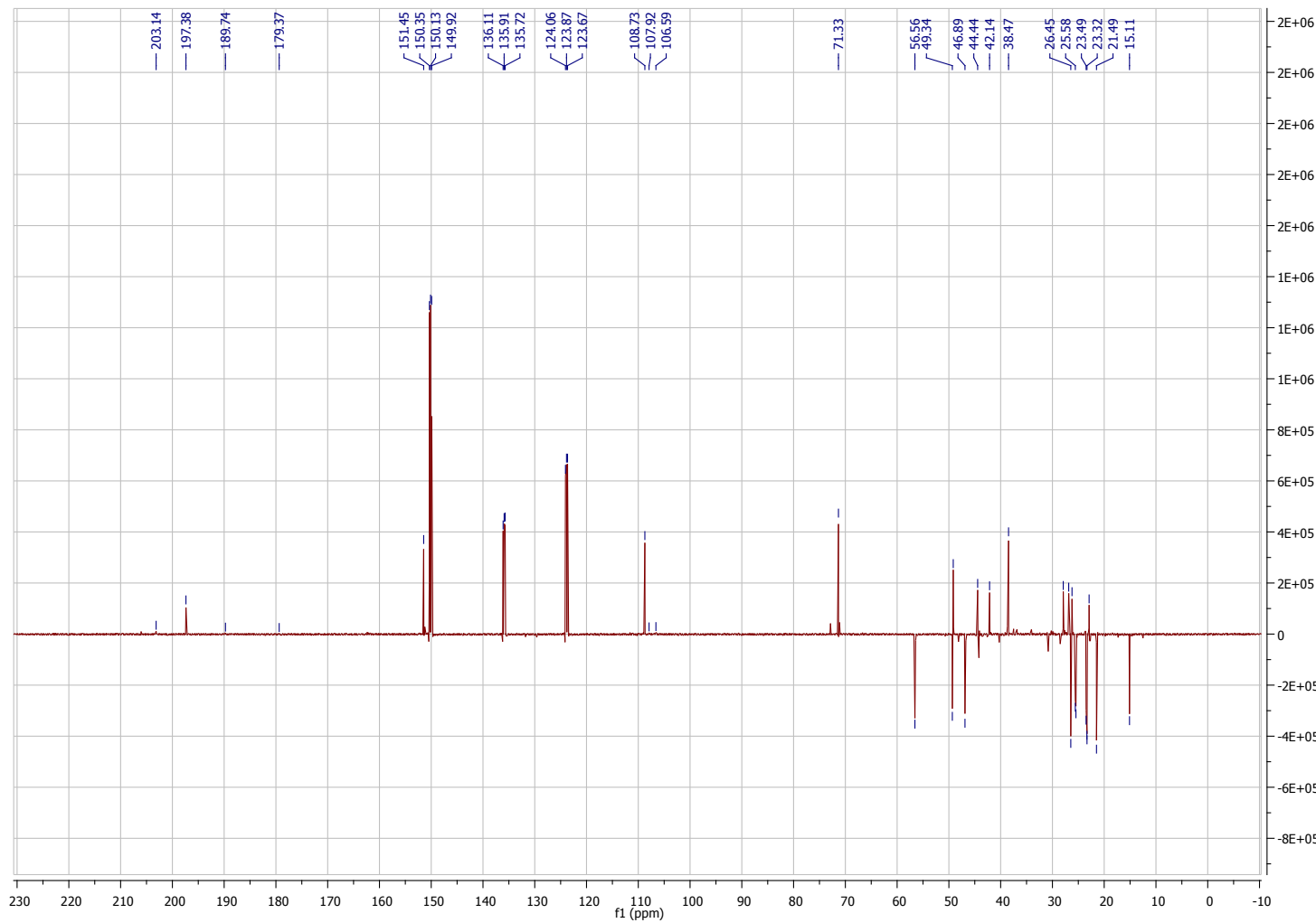
----- CHANNEL f1 -----
NUC1 1H
P1 7.25 usec
PL1 -4.00 dB
PL9 52.77 dB
SF01 500.1324152 MHz

F1 - Acquisition parameters
ND0 1
TD 256
SF01 500.1324 MHz
FIDRES 20.345053 Hz
SW 10.414 ppm
FnMODE States-TPPI

F2 - Processing parameters
SI 2048
SF 500.1299939 MHz
WDW QSINE
SSB 2
LB 0.00 Hz
GB 0
PC 1.00

F1 - Processing parameters
SI 1024
MC2 States-TPPI
SF 500.1299939 MHz
WDW QSINE
SSB 2
LB 0.00 Hz
GB 0

S36. ^{13}C JMOD spectrum of rhodomyrtal C in pyridine- d_5



S37. Theoretical Methodology of CD calculations

To theoretically obtain the ECD spectra of compounds **1**, **2** and **4** we employed the method developed by Brkljača *et al.* (see ref. 9 in the article), where the ECD spectrum arises from a set of representative conformations of the molecule of interest. As the identical procedure was used in the case of both compounds, we present it only for compound **1**.

We first modeled **1** using general AMBER force field (*gaff*).ⁱ The missing parameters, namely the atomic charges, were obtained from the one-conformer RESP fit. The potential was obtained from the HF/6-31G(d) quantum mechanical method, which is consistent with *gaff* methodology. Prior to calculating the electrostatic potential the structure was subject to the optimization also using the HF/6-31G(d) level of theory. All aforementioned calculations were performed using Gaussian 09 package.ⁱⁱ The optimized structures of **1**, **2** and **4** used for their respective RESP fits are shown in the Figure S1 (pdb files of the optimized structures of both compounds can be found at the end of SI), while the found atomic charges are given in Tables S1, S3 and S3, respectively.

Upon solvating compound **1** with 758 molecules of methanol we proceeded with a combination of minimizations and dynamics simulations in explicit solvent (for details consult ref. 10 in the article), which resulted in the equilibrated system at 300 K. The conformational phase space was generated using advanced replica exchange molecular dynamics (REMD), where 16 replicas of the previously equilibrated system

were set on different target temperatures, namely $T = 275, 282, 289, 296.5, 304, 312, 320, 328, 336.5, 345, 354, 363, 372, 381.5, 391$ and 402 K . The temperatures were chosen such that the exchange probability between the replicas falls between 15 and 20 %. The exchanges were attempted every 500 steps. In between, all replicas were subject to Langevin dynamics in the NVT ensemble with 2 fs time step and a collision frequency of 1 ps^{-1} (dynamics was performed with periodic boundary conditions, whereas the long-range electrostatic interactions beyond an 8 Å cutoff were taken into account using the particle mesh Ewald method). The 16 replicas were propagated for a total of 256 ns (16 ns per replica). The coordinates of the entire system were saved every 0.5 ps, which, upon omitting first 2.5 ns from the subsequent analysis (REMD equilibration time), gave rise to 27000 conformations at $T = 296.5\text{ K}$ comprising the conformational space of compound **1**. All molecular dynamics simulations were performed using AMBER 12.ⁱⁱⁱ

The conformational phase space was analyzed by employing principal component analysis (PCA) and clustering (K -means algorithm),^{iv} the latter producing two distinct clusters of conformations (clusters and representative conformations of both compounds are shown in Figure S2). Both the PCA and clustering were based on 10 carbon atoms representing the backbone of compound **1** (Figure S3). Further subclustering of the two clusters (determined on the basis of all atoms) gave rise to 50 conformations representing entire conformational phase space of compound **1**.

The ECD spectra of 50 representative conformations (each classically minimized prior to the spectra calculations) were now calculated using time dependent density functional theory (TDDFT), where B3LYP/6-31+G(d) level of theory was used (first 40 excited states were taken into account). The solvent effect was accounted for by using polarizable continuum model of methanol. Finally, the average ECD spectrum of **1** was obtained as a weighted average of 50 individual spectra, which were prior to the averaging convoluted with Gaussian functions of width 0.18 eV. Thereby, the weight of each individual spectrum was given by the population fraction of the respective subcluster. All ECD spectra calculations were performed using Gaussian 09.³

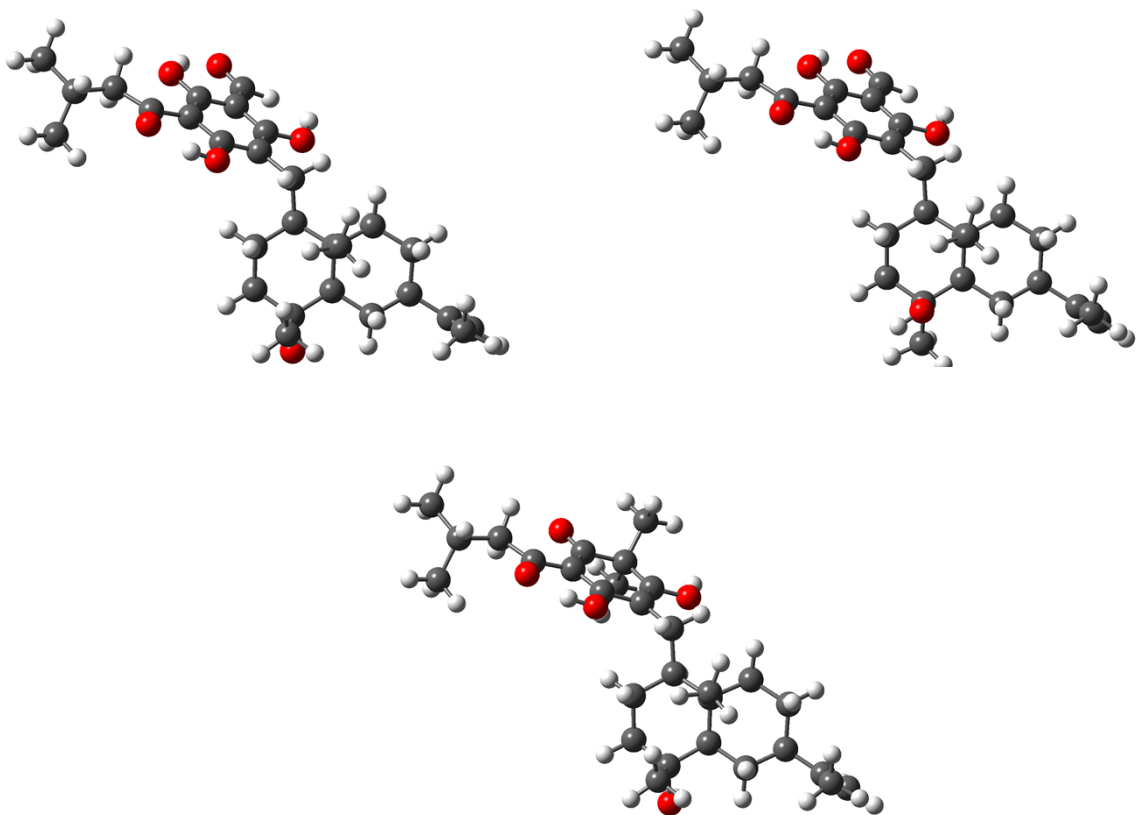


Figure S1. Ball and stick model of the optimized structures of compounds **1** (left), **2** (right) and **4** (bottom), used in their respective one-conformer RESP fits.

Red: oxygen

Table S1. Atom types and corresponding charges in compound **1**

Atom index	Atom type	Charge*	Atom index	Atom type	Charge
1	c3	-0.043330	38	hc	0.020723
2	c3	0.027580	39	c3	-0.034374
3	c3	0.005404	40	hc	0.056408
4	c3	-0.086767	41	hc	0.056408
5	c3	0.030310	42	c2	-0.499713
6	c3	-0.063008	43	ha	0.176411
7	hc	0.012136	44	ha	0.176411
8	hc	0.012136	45	ca	0.011809
9	hc	0.057508	46	ca	0.131985
10	hc	0.057508	47	ca	0.039116
11	hc	0.034749	48	ca	-0.113902
12	hc	0.033922	49	ca	-0.109859
13	hc	0.033922	50	ca	0.132682
14	hc	0.014281	51	oh	-0.461228
15	c3	0.150367	52	ho	0.429760
16	c3	0.002352	53	oh	-0.522078
17	c3	-0.132752	54	ho	0.441642
18	c3	-0.048318	55	oh	-0.478001
19	hc	0.032749	56	ho	0.446908
20	hc	0.032749	57	c	0.444498
21	hc	0.059601	58	o	-0.544321
22	hc	0.049725	59	h4	0.038703
23	hc	0.049725	60	c	0.498587
24	oh	-0.650855	61	o	-0.538856
25	ho	0.408811	62	c3	-0.072597
26	c2	0.023115	63	hc	0.035814
27	c3	-0.077207	64	hc	0.035814
28	hc	0.039444	65	c3	0.228027
29	hc	0.039444	66	hc	-0.010587
30	hc	0.039444	67	c3	-0.214888
31	c3	-0.070294	68	hc	0.044949
32	hc	0.040870	69	hc	0.044949
33	hc	0.040870	70	hc	0.044949
34	hc	0.040870	71	c3	-0.214888
35	c3	-0.094613	72	hc	0.044949
36	hc	0.020723	73	hc	0.044949
27	hc	0.020723	74	hc	0.044949

Table S2. Connectivity table for compound **1**

AI1 ^a	AI2 ^b	AI1	AI2
1	2	35	37
1	6	35	38
1	7	39	40
1	8	39	41
2	3	39	45
2	16	42	43
2	35	42	44
3	4	45	46
3	14	45	47
3	15	45	61
4	5	46	48
4	9	46	51
4	10	47	49
5	6	47	53
5	11	48	50
5	26	48	60
6	12	49	50
6	13	49	57
15	18	50	55
15	24	51	52
15	31	53	54
16	17	55	56
16	21	57	58
16	39	57	59
17	18	60	61
17	22	60	62
17	23	62	63
18	19	62	64
18	20	62	65
24	25	65	66
26	27	65	67
26	42	65	71
27	28	67	68
27	29	67	69
27	30	67	70
31	32	71	72
31	33	71	73
31	34	71	74
35	36		

^aAtomic index of the first atom involved in the bond.^bAtomic index of the second atom involved in the bond.

Table S3. Atom types and corresponding charges in compound 2

Atom index	Atom type	Charge*	Atom index	Atom type	Charge
1	c3	-0.080121	38	ha	0.176164
2	c3	0.039965	39	ca	0.003487
3	c3	0.017725	40	ca	0.143604
4	c3	-0.194294	41	ca	0.034346
5	c3	0.037094	42	ca	-0.112734
6	c3	-0.041422	43	ca	-0.108830
7	hc	0.014233	44	ca	0.128528
8	hc	0.014233	45	oh	-0.480174
9	hc	0.100510	46	ho	0.439569
10	hc	0.100510	47	oh	-0.508307
11	hc	0.039736	48	ho	0.436063
12	hc	0.030324	49	oh	-0.477005
13	hc	0.030324	50	ho	0.446515
14	hc	0.034549	51	c	0.445932
15	c3	0.168587	52	o	-0.546229
16	c3	0.025220	53	h4	0.038018
17	c3	-0.078476	54	c	0.498750
18	c3	0.022494	55	o	-0.543206
19	hc	-0.007133	56	c3	-0.076268
20	hc	-0.007133	57	hc	0.035137
21	hc	0.044257	58	hc	0.035137
22	hc	0.035149	59	c3	0.243092
23	hc	0.035149	60	hc	-0.014334
24	c2	0.012115	61	c3	-0.214823
25	c3	-0.075762	62	hc	0.043673
26	hc	0.041245	63	hc	0.043673
27	hc	0.041245	64	hc	0.043673
28	hc	0.041245	65	c3	-0.214823
29	c3	-0.054614	66	hc	0.043673
30	hc	0.020881	67	hc	0.043673
31	hc	0.020881	68	hc	0.043673
32	hc	0.020881	69	c3	-0.044865
33	c3	-0.030780	70	hc	0.008195
34	hc	0.049895	71	hc	0.008195
35	hc	0.049895	72	hc	0.008195
36	c2	-0.500983	73	oh	-0.706359
37	ha	0.176164	74	ho	0.463210

Table S4. Connectivity table for compound **2**

AI1 ^a	AI2 ^b	AI1	AI2
1	2	33	35
1	6	33	39
1	7	36	37
1	8	36	38
2	3	39	40
2	16	39	41
2	29	40	42
3	4	40	45
3	14	41	43
3	15	41	47
4	5	42	44
4	9	42	54
4	10	43	44
5	6	43	51
5	11	44	49
5	24	45	46
6	12	47	48
6	13	49	50
15	18	51	52
15	69	51	53
15	73	54	55
16	17	54	56
16	21	56	57
16	33	56	58
17	18	56	59
17	22	59	60
17	23	59	61
18	19	59	65
18	20	61	62
24	25	61	64
24	36	65	66
25	26	65	67
25	27	65	68
25	28	69	70
29	30	69	71
29	31	69	72
29	32	73	74
33	34		

^aAtomic index of the first atom involved in the bond.

^bAtomic index of the second atom involved in the bond.

Table S5. Atom types and corresponding charges in compound 4

Atom index	Atom type	Charge*	Atom index	Atom type	Charge
1	c3	-0.045081	40	hc	0.085842
2	c3	0.031947	41	hc	0.085842
3	c3	0.008017	42	ce	-0.009628
4	c3	-0.078380	43	ce	0.144413
5	c3	0.016502	44	c2	0.125849
6	c3	-0.057243	45	cf	-0.147667
7	hc	0.015018	46	c3	0.151798
8	hc	0.015018	47	c	0.243101
9	hc	0.057612	48	oh	-0.622375
10	hc	0.057612	49	ho	0.503537
11	hc	0.036096	50	oh	-0.412296
12	hc	0.033573	51	ho	0.410493
13	hc	0.033573	52	c3	-0.031481
14	hc	0.018040	53	hc	0.018267
15	c3	0.134742	54	hc	0.018267
16	c3	-0.011691	55	hc	0.018267
17	c3	-0.154139	56	c3	-0.031481
18	c3	-0.040418	57	hc	0.018267
19	hc	0.036476	58	hc	0.018267
20	hc	0.036476	59	hc	0.018267
21	hc	0.050939	60	o	-0.486904
22	hc	0.061484	61	c	0.412391
23	hc	0.061484	62	o	-0.530411
24	oh	-0.650248	63	c3	-0.053758
25	ho	0.409153	64	hc	0.061562
26	c2	0.025514	65	hc	0.061562
27	c3	-0.078522	66	c3	0.187942
28	hc	0.039675	67	hc	0.000236
29	hc	0.039675	68	c3	-0.227497
30	hc	0.039675	69	hc	0.048500
31	c3	-0.063165	70	hc	0.048500
32	hc	0.039898	71	hc	0.048500
33	hc	0.039898	72	c3	-0.227497
34	hc	0.039898	73	hc	0.048500
35	c3	-0.084913	74	hc	0.048500
36	hc	0.019119	75	hc	0.048500
37	hc	0.019119	76	c2	-0.495564
38	hc	0.019119	77	ha	0.175099
39	c3	-0.120360	78	ha	0.175099

Table S6. Connectivity table for compound 4

AI1 ^a	AI2 ^b	AI1	AI2
1	2	35	38
1	6	39	40
1	7	39	41
1	8	39	42
2	3	42	43
2	16	42	44
5	13	43	45
2	35	43	50
3	4	44	46
3	14	44	48
3	15	45	47
4	5	45	61
4	9	46	47
4	10	46	52
5	6	46	56
5	11	47	60
5	26	48	49
6	12	50	51
6	13	52	53
15	18	52	54
15	24	52	55
15	31	56	57
16	17	56	58
16	21	56	59
16	39	61	62
17	18	61	63
17	22	63	64
17	23	63	65
18	19	63	66
18	20	66	67
24	25	66	68
26	27	66	72
26	76	68	69
27	28	68	70
27	29	68	71
27	30	72	73
31	32	72	74
31	33	72	75
31	34	76	77
35	36	76	78
35	37		

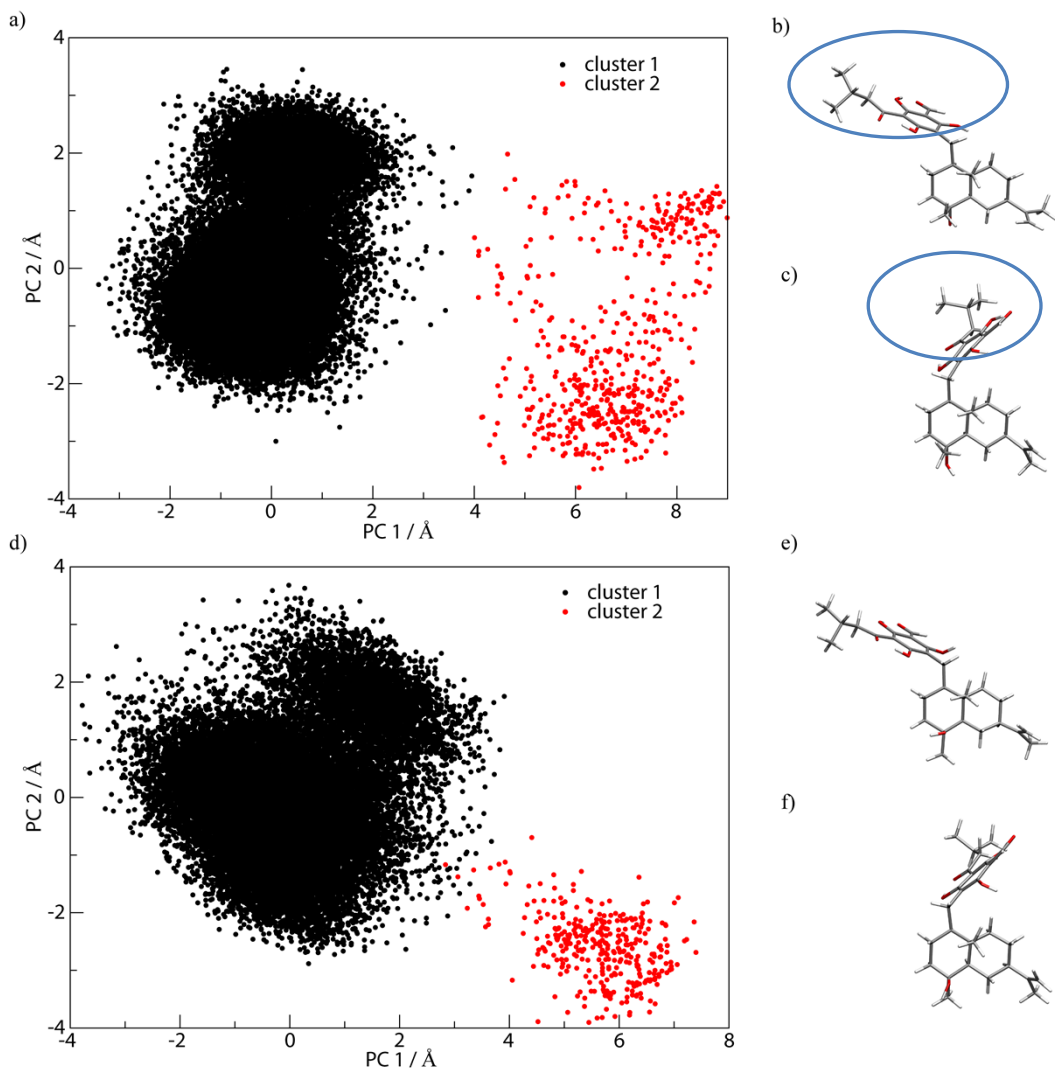


Figure S2. a) Conformations of compound **1** simulated in methanol are projected onto first two principle component vectors found using PCA (analysis is based on ten carefully chosen C atoms, see Figure S3). Clustering produced two distinct clusters, shown in black and red, with cluster **1** representing the vast majority of the conformations (more than 95 % of all conformations belong to this cluster). The main difference between the conformations belonging to cluster 1 and 2 can be found by inspecting the representative conformations (structures with the lowest rms deviation from the relevant centroid) of the respective clusters. b) The representative conformation of cluster 1. c) The representative

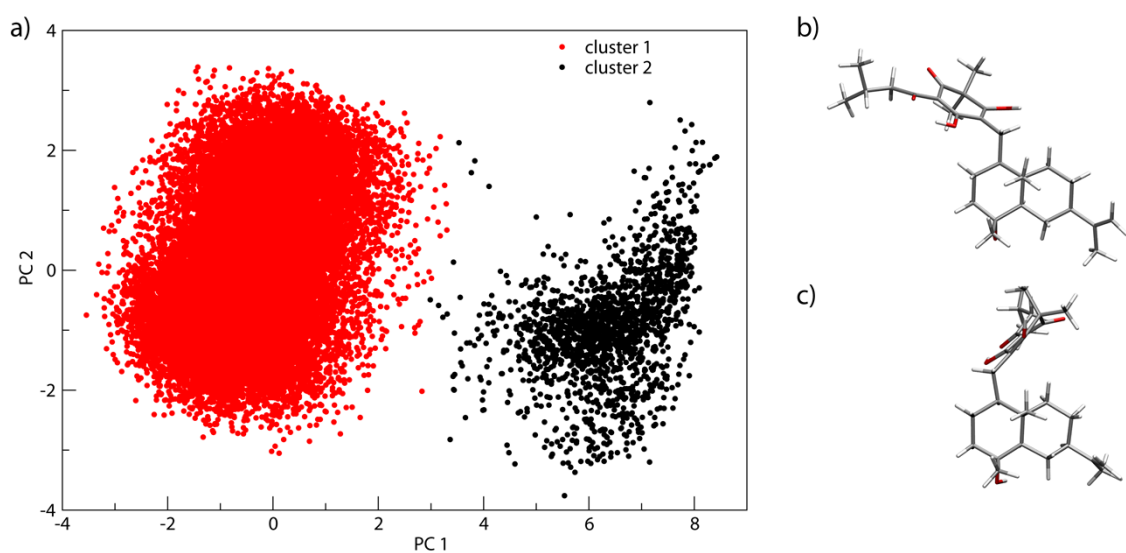


Figure S3. a) Conformations of compound 4 simulated in methanol are projected onto first two principle component vectors found using PCA (analysis is based on ten carefully chosen C atoms, see Figure S5). Clustering produced two distinct clusters, shown in red and black. Cluster 1 (red) represents the vast majority of conformations, with 90.58 % of all conformations belonging to it. The remaining conformations (9.42 %) belong to smaller cluster 2 (black). The main difference between the conformations belonging to cluster 1 and 2 can be found by inspecting the representative conformations (structures with the lowest rms deviation from the relevant centroid) of the respective clusters. b) The representative conformation of cluster 1. c) The representative conformation of cluster 2. The main difference between the two representative conformations is the relative position of the dominant side chain (enclosed in blue ellipses) to the trans-decalin moiety in compound 1, as can be observed from b) and c).

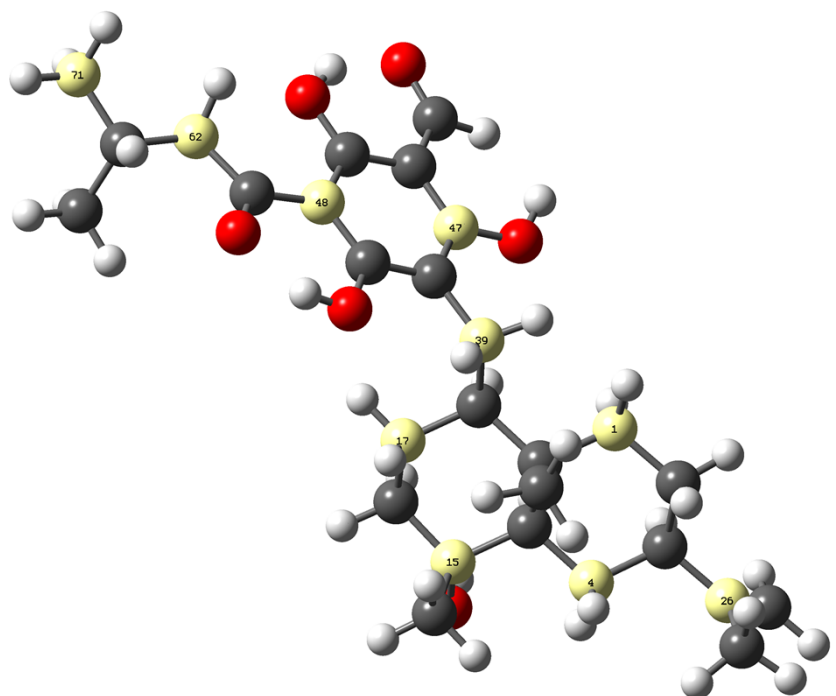


Figure S4. Set of ten carbon atoms on which PCA and clustering of the compound **1** were based are shown in yellow, together with their respective atom indices (the indices, in ascending order, are 1, 4, 15, 17, 26, 39, 47, 48, 62, 71. For details consult Tables S1 and S2). The equivalent set of atoms was chosen for the analysis of the compound **2** (atom indices of these ten atoms, in the ascending order, are 1, 4, 15, 17, 24, 33, 41, 42, 56, 65. For details consult Tables S3 and S4).

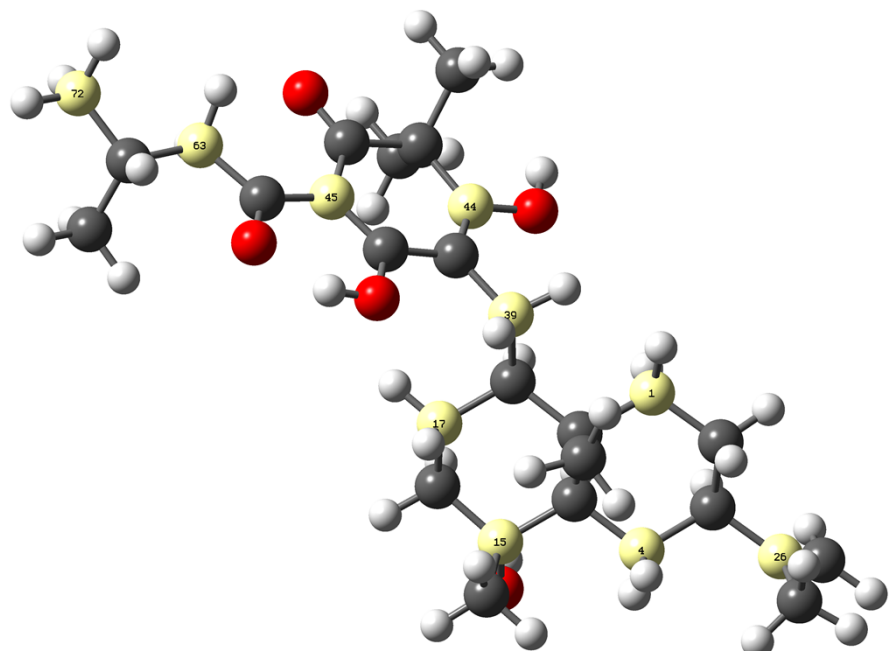


Figure S5. Set of ten carbon atoms on which PCA and clustering were based are shown in yellow, together with their respective atom indices (the indices, in ascending order, are 1, 4, 15, 17, 26, 39, 44, 45, 63, 72. For details consult tables S5 and S6).

-
- (i) Wang, J.; Wolf, R. M.; Caldwell, J. W.; Kollman, P. A.; Case, D. A. *J. Comput. Chem.* **2004**, *25*, 1157.
- (ii) Frisch, M. J.; Trucks, G. W.; Schlegel, H. B.; Scuseria, G. E.; Robb, M. A.; Cheeseman, J. R.; Scalmani, G.; Barone, V.; Mennucci, B.; Petersson, G. A.; Nakatsuji, H.; Caricato, M.; Li, X.; Hratchian, H. P.; Izmaylov, A. F.; Bloino, J.; Zheng, G.; Sonnenberg, J. L.; Hada, M.; Ehara, M.; Toyota, K.; Fukuda, R.; Hasegawa, J.; Ishida, M.; Nakajima, T.; Honda, Y.; Kitao, O.; Nakai, H.; Vreven, T.; Montgomery, Jr., J. A.; Peralta, J. E.; Ogliaro, F.; Bearpark, M.; Heyd, J. J.; Brothers, E.; Kudin, K. N.; Staroverov, V. N.; Kobayashi, R.; Normand, J.; Raghavachari, K.; Rendell, A.; Burant, J. C.; Iyengar, S. S.; Tomasi, J.; Cossi, M.; Rega, N.; Millam, N. J.; Klene, M.; Knox, J. E.; Cross, J. B.; Bakken, V.; Adamo, C.; Jaramillo, J.; Gomperts, R.; Stratmann, R. E.; Yazyev, O.; Austin, A. J.; Cammi, R.; Pomelli, C.; Ochterski, J. W.; Martin, R. L.; Morokuma, K.; Zakrzewski, V. G.; Voth, G. A.; Salvador, P.; Dannenberg, J. J.; Dapprich, S.; Daniels, A. D.; Farkas, Ö.; Foresman, J. B.; Ortiz, J. V.; Cioslowski, J.; Fox, D. J. *Gaussian 09, Revision A.02*, Gaussian, Inc., Wallingford CT, 2009.
- (iii) Case, D. A.; Darden, T. A.; Cheatham, T. E. III; Simmerling, C. L.; Wang, J.; Duke, R. E.; Luo, R.; Walker, R. C.; Zhang, W.; Merz, K. M.; Roberts, B.; Hayik, S.; Roitberg, A.; Seabra, G.; Swails, J.; Götz, A. W.; Kolossváry, I.; Wong, K. F.; Paesani, F.; Vanicek, J.; Wolf, R. M.; Liu, J.; Wu, X.; Brozell, S. R.; Steinbrecher, T.; Gohlke, H.; Cai, Q.; Ye, X.; Wang, J.; Hsich, M.-J.; Cui, G.; Roe, D. R.; Mathews, D. H.; Seetin, M. G.; Salomon-Ferrer, R.; Sagui, C.; Babin, V.; Luchko, T.; Gusarov, S.; Kovalenko, A.; Kollman, P. A. (2012), AMBER 12, University of California, San Francisco.
- (iv) Shao, J.; Tanner, S. W.; Thompson, N.; Cheatham, T. E. III. *J. Chem. Theory Comput.* **2007**, *3*, 2312.